

Article

# Non-Mineralized Fossil Wood

George E. Mustoe 

Geology Department, Western Washington University, Bellingham WA 98225, USA; mustoeg@wwu.edu;  
Tel.: +1-360-650-3582

Received: 25 May 2018; Accepted: 11 June 2018; Published: 18 June 2018



**Abstract:** Under conditions where buried wood is protected from microbial degradation and exposure to oxygen or harsh chemical environments, the tissues may remain unmineralized. If the original organic matter is present in relatively unaltered form, wood is considered to be mummified. Exposure to high temperatures, whether from wild fires or pyroclastic flows, may cause wood to be converted to charcoal. Coalification occurs when plant matter undergoes gradual metamorphosis, producing bituminous alteration products. Examples of all three types of non-mineralized wood are common in the geologic record. This report describes some of the most notable occurrences, reviews past research and introduces data from several localities in North America.

**Keywords:** fossil wood; carbonized; charcoal; coalified; mummified; paleobotany

## 1. Introduction

From a deep time perspective, forests are a transient phenomenon, their existence depending on environmental factors that include elevation change, atmospheric physics, ocean currents patterns, and tectonic plate motion. These factors determine whether a region is an arid desert or a lush rainforest. Foresters describe forests that contain trees with ages of only a few hundred years as “old growth”. The oldest known age record for an individual tree is a Bristlecone Pine (*Pinus longaeva*) growing in White Mountains of California USA; a tree core taken in 2012 was observed to have 5067 annual rings [1]. The ages of clonal tree clusters, where individual trunks share a common root network, may be much greater, e.g. the 80,000 year age estimated for ~47,000 component trees of a Quaking Aspen (*Populus tremuloides*) grove in central Utah, USA [2]. The ages of these living trees are brief in comparison to fossil evidence of trees that comprised ancient forests. The infiltration and replacement of inorganic minerals produces petrified wood that has sufficient durability to be preserved for many millions of years. Recent reports [3,4] describe these mineralization processes in detail, and list earlier literature. Less well-known are fossil forests where ancient trees have been preserved as original tissue, or as organic material that has undergone structural alteration.

This paper provides a detailed review of fossil wood occurrences where tissues have not been mineralized. These fossils are sometimes described as “carbonized wood”, but unmineralized ancient wood can be divided into three categories. Mummified wood consists of original tissues that may have undergone anatomical distortion or desiccation, but which are otherwise free of alteration. Charcoalified wood originates when wood is combusted in an anaerobic environment, causing much of the organic materials to be reduced to pure carbon. Coalified wood consists of tissues that have been altered by heat and pressure during deep burial, converting the original organic constituents to a mixture of pure carbon and various hydrocarbons.

## 2. Analytical Methods

Scanning electron microscope (SEM) images were taken by the author using a Tescan Vega SEM at Western Washington University, Bellingham, WA USA.

### 3. Mummified Wood

A common question asked of fossil wood researchers is “how long does it take for wood to become petrified?” There is no uniform answer, because fossilization processes are highly variable. In siliceous hot springs, wood may become rapidly impregnated with silica [3,5–7], but in other environments, buried wood may be preserved for tens of millions of years without experiencing mineralization. The most important conditions required for mummification are an absence of microbial and chemical degradation, and burial conditions where mineral-bearing groundwater is unable to penetrate the tissues. Mummified wood consists of original tissues that have undergone minimal degradation of cellular constituents. This preservation is a result of several factors: inhibition of wood-destroying microbes, decreased oxygen availability, and the absence of harsh chemical or physical conditions (e.g., high alkalinity or acidity, or elevated temperatures). Environments that favor mummification include deeply submerged wood, burial in impermeable sediments, aridity, or low temperatures [8–12]. Lignin and cellulose, the primary constituents of wood, may undergo alteration on a microscopic level, even though the overall appearance of the ancient wood may appear unchanged. Wood cell walls consist of an outer primary wall that encloses a multilayered secondary wall. The primary wall, which may be relatively thick, consists mostly of cellulose and hemicellulose, in contrast to the thinner secondary wall that is largely composed of a mixture of cellulose and lignin. This secondary wall commonly consists of three discrete layers (lamellae) that differ in the orientation of their cellulosic aggregates and the degree of lignification. Microbial degradation of wood may result in destruction of the wood sugars cellulose and hemicellulose, resulting in relative enrichment of lignin [13,14]. Deterioration of the lignin-rich secondary wall may not greatly disrupt the overall cellular architecture as long as the cellulosic outer walls remain relatively intact (Figure 1). When it is preserved, cellulose has scientific value because carbon and oxygen isotope ratios in this substance can be used to estimate paleoprecipitation and paleotemperature [15–18].

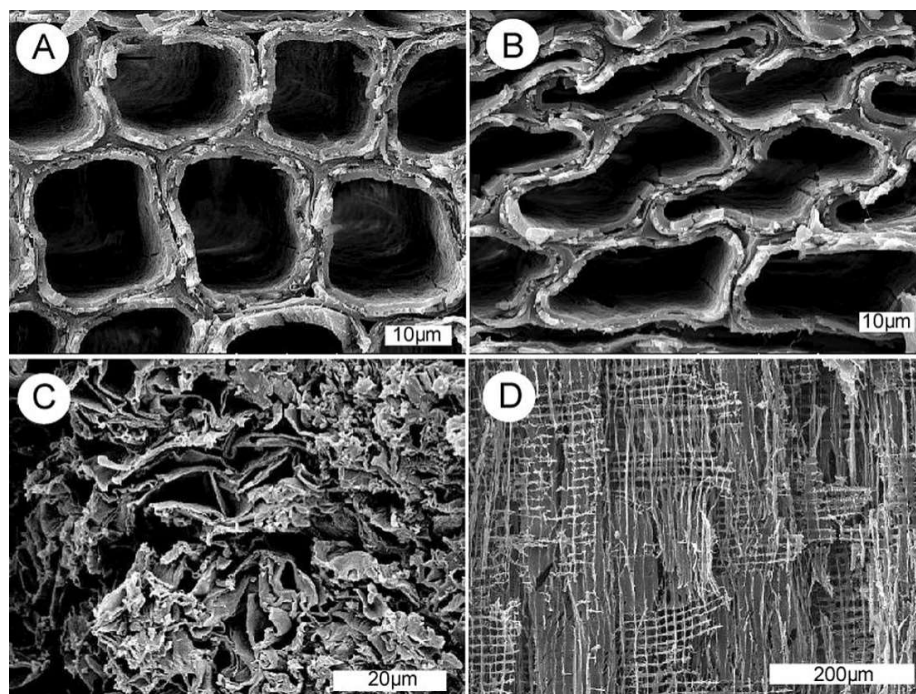


**Figure 1.** Anatomical preservation in mummified wood from western Washington, USA. (A,B) Transverse views, late Pleistocene wood, Whidbey Formation, Swantown, Whidbey Island, Island County, Washington State, USA. (C) Transverse view, Wilkes Formation compressed wood. (D) Late Pleistocene wood showing extensive decay. Radial view. Net-like structures are relict ray cell walls, Whidbey Formation, Cama Beach, Camano Island, Island County, Washington, USA.

Reported occurrences of mummified wood range in age from Paleocene to Holocene. This subfossil wood is often locally abundant, particularly in Quaternary deposits, where glacial, fluvial, and volcanoclastic lahar deposits provide deep layers of fine sediment that preserve organic materials. The following section describes some of the best-known localities, but it is not a comprehensive list.

### 3.1. Canadian Arctic Localities

Spectacular examples of mummified wood occur in the Canadian Arctic, ranging in age from Paleocene to Pliocene (Figure 2). Although the modern High Arctic is a polar desert typified by long cold winters and short cool summers, early Tertiary conditions were very different, with a warm ice-free environment where plants benefited from high humidity and a growing season that had three months of continuous light. Three months of continuous darkness during Arctic Circle winters favored conifers rather than angiosperms. These fossil forests are typically dominated by *Metasequoia*, an unusual deciduous conifer particularly suited for long dark winters. Many other taxa are represented, particularly in the Miocene and Pliocene occurrences [19,20].

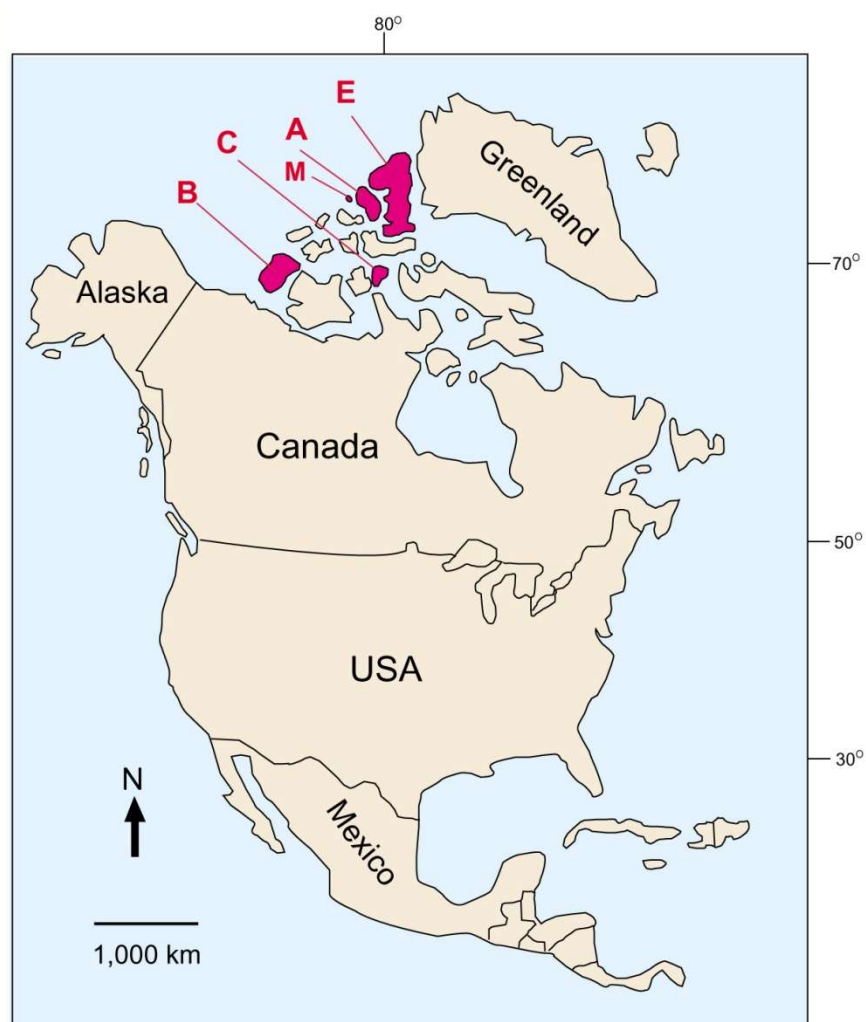


**Figure 2.** Fossil forests in the Canadian Arctic. (A) Axel Heiberg Island (Eocene); (B) Banks Island (Miocene/Pliocene); (C) Cornwallis Island (Miocene); (E) Ellesmere Island (Paleocene/Eocene, Pliocene); (M) Meighen Island (Miocene).

### 3.2. Ellesmere Island—Late Paleocene/early Eocene, Pliocene

Fossil wood was discovered at northern Ellesmere Island in 1883 at a site later described as “Brainard’s Petrified Forest”, named after a Sargent D.L. Brainard, a survivor of the ill-fated Greely Expedition of 1881–1883 [21]. Interest was revived in the 1980s when Geological Survey of Canada geologist Neil McMillan observed fossil wood at Ellesmere Island. The main fossil forest areas at Strathcona and Stenkul Fjords contain siderite-mineralized wood preserved in Late Paleocene–Early Eocene coal-bearing sediments of the Iceberg Bay Formation [22–24]. Pliocene mummified wood occurs at the Beaver Pond fossil site near the head of Strathcona Fjord, where braided river deposits of the Beaufort Formation preserve woody debris [25]. Many of the twigs have teeth marks left by ancestral beaver (Figure 3). Pliocene wood also occurs at nearby Meighen Island, including both individual logs and fine woody debris [26].

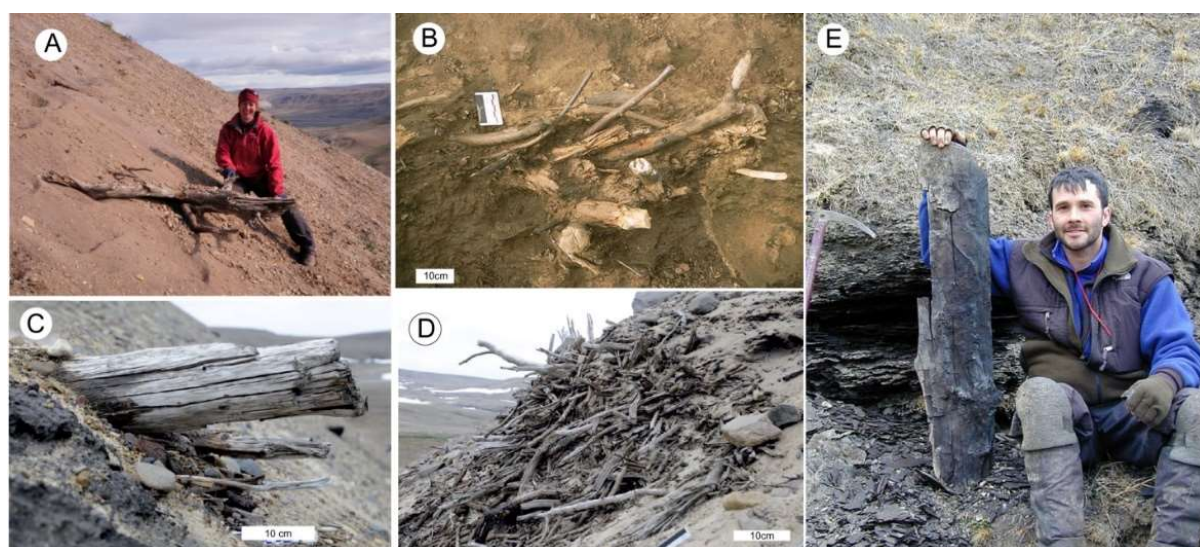


**Figure 3.** Pliocene wood from Canadian Arctic sites. (A) Natalia Rybcynski with log, Fyles Leaf Bed, ~3 km south of Beaver Pond locality, Ellesmere Island. (B) Beaver-gnawed twigs preserved in Pliocene sediments at Beaver Pond site. (C) Tree trunk in Beaufort Fm. Strata at Meighen Island. (D) Fine woody debris, Meighen Island. Photos courtesy of Natalia Rybcynski. (E) William Hagopian with freshly excavated trunk fragment, Stenkul Fjord, Ellesmere Island 2005. Photo by Ann Jefferson.

### 3.3. Axel Heiberg Island—Middle Eocene

The fossil forest on this island was discovered in 1985 by helicopter pilot Paul Tudge, who had been transporting Canadian Geological Survey scientists to Arctic locations for years. Tudge notified University of Saskatchewan paleobotanist James Basinger, who organized the first expeditions to visit the site.

Located in the Geodetic Hills, the fossil forest is preserved in sediments of the middle Eocene Buchanan Lake Formation. The fossils are preserved in a basin where fluvial sedimentation included episodic floods that killed trees, burying stumps in situ together with fallen logs and abundant forest floor leaf litter. The total depth of sediment exceeds 150 m, and preserves at least 33 separate fossil-bearing layers [27]. As noted later in this report, although mummified wood is a dominant component of the Axel Heiberg Island fossil forest, some specimens have been coalified.

*Metasequoia* (Dawn Redwood) wood is by far the most abundant fossil (Figure 4). Other conifers include fir, cypress, ginkgo, larch, redwood, spruce, pine and hemlock; Angiosperm trees include maple, alder, birch, hickory, chestnut, beech, ash, holly, walnut, sweetgum, sycamore, oak, willow, and elm. Herbaceous plants are represented by honeysuckle and sumac; other taxa include several species of ferns and mosses [27]. This botanical diversity is evidence of a taxonomically diverse

ecosystem, where plant communities flourished in a continually-changing floodplain environment. Despite the rigors of conducting research in a remote location with a harsh modern polar climate, the Axel Heiberg fossil forest has been the subject of enthusiastic scientific inquiry. Published research includes general descriptions [19,22,28–32], as well as more specialized reports. These include analyses of paleoclimate and paleoecology [15,18,33–40], and plant anatomy and taxonomy [14,41–43].

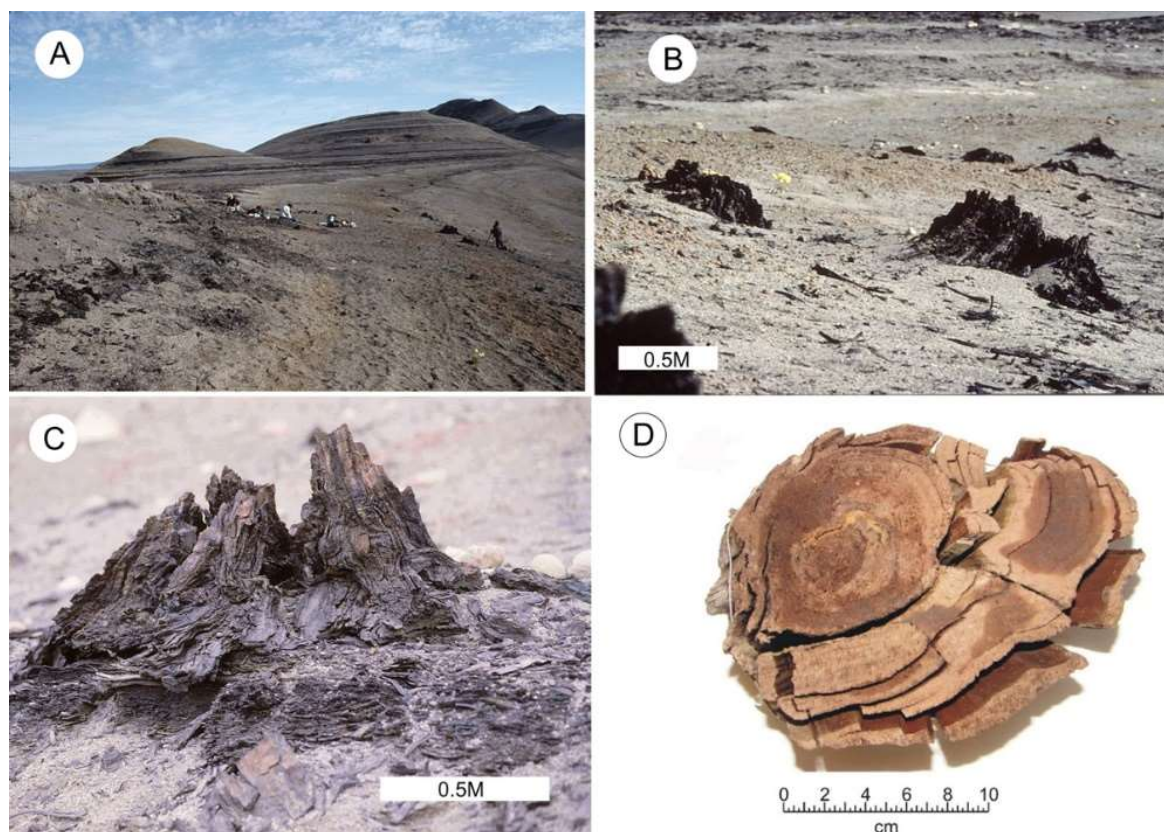


**Figure 4.** Axel Heiberg Island, Canadian Arctic. (A) Geodetic Hills site, 1999. (B) *Metasequoia* stumps exposed by weathering. Photos courtesy of David Greenwood. (C) *Metasequoia* stump, 2000, photo by William Hagopian. (D) Close view of *Metasequoia* wood, showing annual rings and desiccation fractures. Photo from Kaelin et al. [44].

#### 3.4. Banks Island—Middle Miocene-Pliocene

At Banks Island, the Miocene Ballast Brook Formation consists of sediments deposited on an ancient floodplain, where an upper peat layer preserves cones, foliage, twigs, and logs (Figure 5) [45]. In situ stumps are exposed at the top of the peat player; logs buried in the peat lie adjacent to their corresponding stumps [46]. Separated by an unconformity, the overlying Beaufort Formation is a Pliocene braided river deposit where logs and woody debris are preserved as transported material (Williams 2006. Williams et al. 2008). Paleobotanical studies date to the 1960s, when University of Alberta professor Len Hills began studying Banks Island plant fossils [47–50].

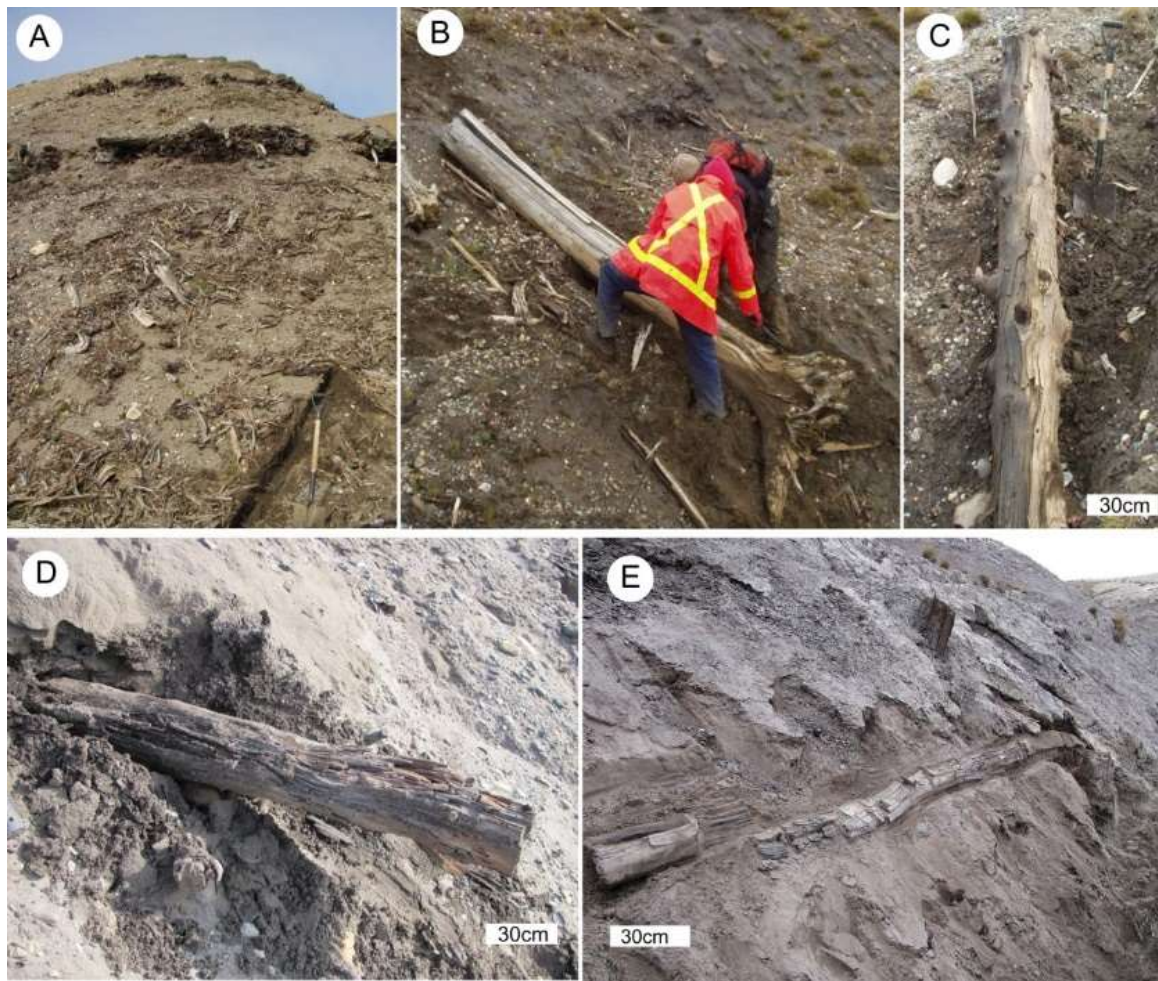


**Figure 5.** Miocene Beaufort Formation at Ballast Brook, Banks Island, Canadian Arctic. (A) General site view. (B) Tree trunk with intact root crown. (C) Excavated trunk showing branching. 2005 photos courtesy of Christopher J. Williams. (D,E) Partially exposed logs, 2010, photos courtesy of William Hagopian.

### 3.5. Cornwallis Island—Miocene

A single sample of mummified collected from a roadcut at Resolute has been described as having elevated levels of Ca, Fe, and S relative to modern wood, but scanning and transmission electron microscopy show no evidence of mineralization [14].

### 3.6. Northwestern Canada

Late Paleocene/early Eocene woods have been preserved in volcanoclastic material filling the upper zones of kimberlite pipes in the Lac de Gras region of Slave Province, Canada, the site of many open pit diamond mines (Figure 6). The wood is inferred to represent a tree from the boreal forest surrounding the eruption zone, where a trunk collapsed into the diatreme, becoming preserved in the sterile environment of the volcanoclastic kimberlite. Other mummified woods have been recovered from another diamond mine in the same region [51]. Cellulose  $\delta^{13}\text{C}$ ,  $\delta^{18}\text{O}$  and  $\delta^2\text{H}$  values indicate the Paleogene climate of the Canadian subarctic was 12–17 °C warmer and four times wetter than present [52,53].

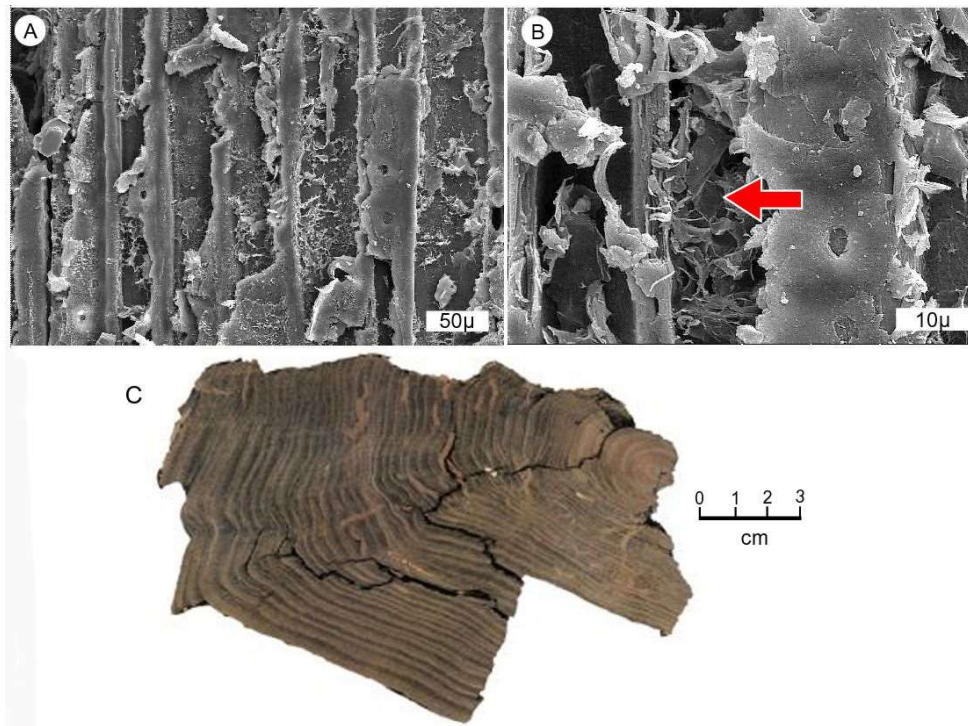


**Figure 6.** Paleocene/Eocene mummified wood from kimberlite pipes, Subarctic Canada. (A,B) *Metasequoia* heartwood showing tyloses (arrow), Panda Pipe Ekati Diamond Mine. Specimen provided by Alex Wolfe. (C) *Piceaoxylon* from Diavik Diamond Mine. Photo by Benjamin Hook [52].

### 3.7. United States of America

Mummified wood occurs in many locations, particularly in Pleistocene and Holocene sediments. Examples where intact logs are preserved include the Farmdale Geosol in Illinois [54] and Mt. Pleasant Bluff, Louisiana [55]. This report focuses on three locations that offer notable examples of wood mummification that range in age from late Miocene to late Pleistocene (Figure 7).

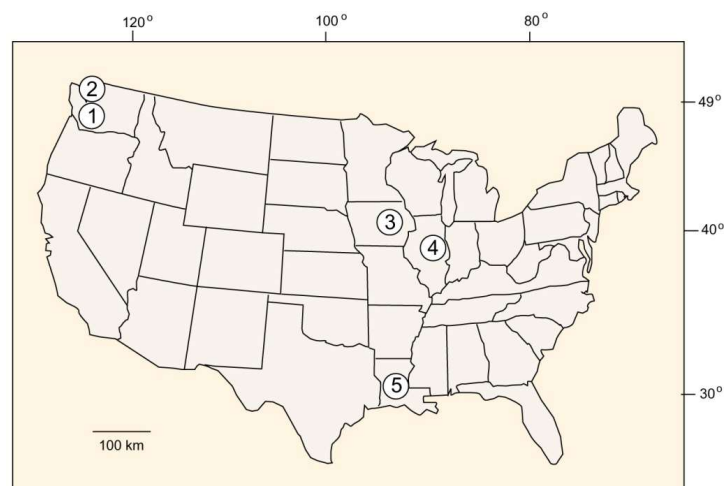


**Figure 7.** Mummified wood localities in USA. (1) Wilkes Formation, Washington, late Miocene. (2) Northern Puget Sound, Washington, late Pleistocene. (3) Two Creeks Forest, Wisconsin, late Pleistocene. (4) Farmdale Geosol, Illinois, late Pleistocene. (5) Mt. Pleasant Bluff, Louisiana, late Pleistocene.

### 3.8. Wilkes Formation, Washington, USA—Late Miocene

The Wilkes formation consists of a stacked series of volcanic mudflow (lahar) sediments that episodically inundated a lowland forest, alternating with lacustrine strata that were deposited during quiescent intervals. Abundant mummified wood is evidence of paleoenvironment: upright stems where mudflows buried living vegetation (Figure 8A), and layers of woody peat that represents organic debris transported by the mudflow (Figure 8B). Radiometric dating of a tephra interbed gave a Late Miocene age of  $6.13 \pm 0.08$  Ma [56]. Taxonomy of the wood has not been attempted, but fossil pollen provides evidence of a swamp forest dominated by *Taxodium* (Swamp Cypress) and *Nyssa* (Tupelo), with diverse angiosperms as minor constituents [57].

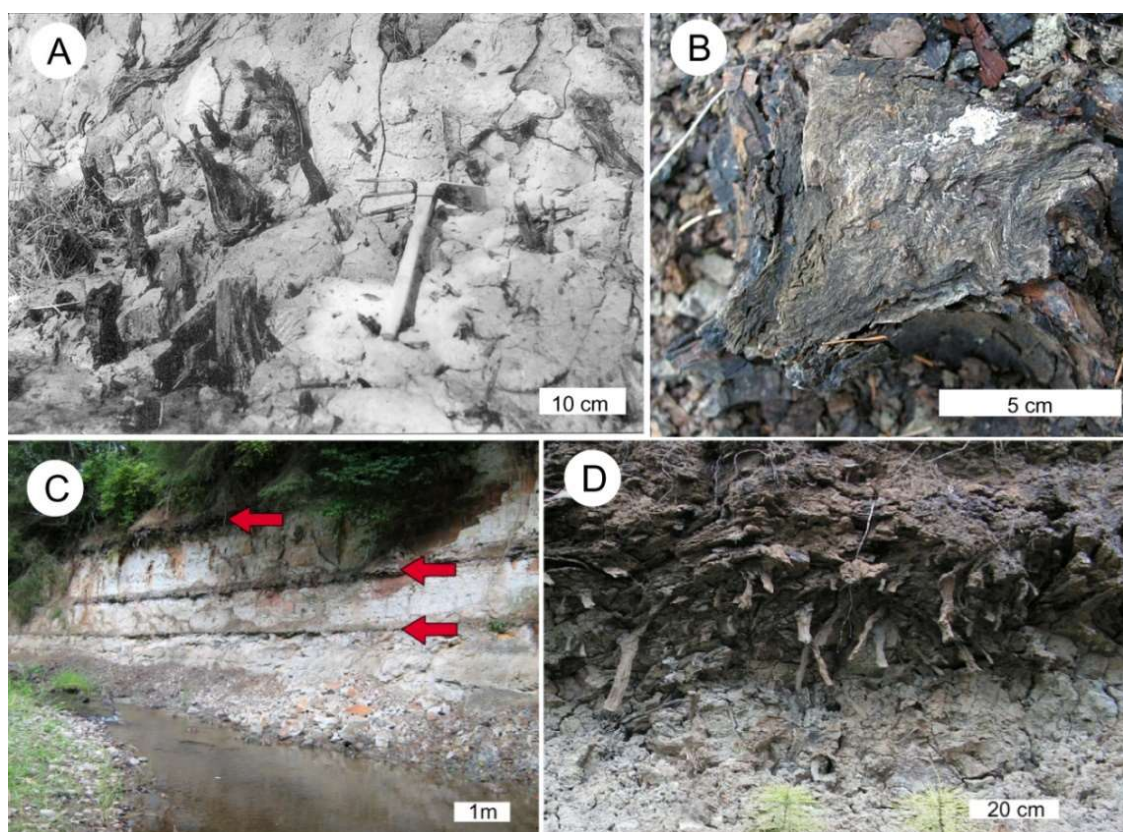


**Figure 8.** Miocene mummified wood in Wilkes Fm. Strata at Salmon Creek, Lewis County, Washington, USA. (A) Upright stems buried by volcanic mudflow. (B) Transverse view of in situ stump, showing compression of original circular shape and deformation of annual rings. (C) Three thin wood mat layers separated by thin mudflow sediments. (D) Close view of the lowest wood mat, showing flattening of individual stems.

Preservation quality of the wood is variable, typically consisting of wood that has been compressed from burial pressure, and deformed by desiccation. Exposure to weathering causes many mummified specimens to be shattered (Figure 9A,B), but intact specimens can be found (Figure 9C). Brown mummified wood is abundant (Figure 9D), as well as wood that has been partially coalified (Figure 9E,F). Even in the freshest-looking specimens, tissues commonly show structural damage (Figure 1C).

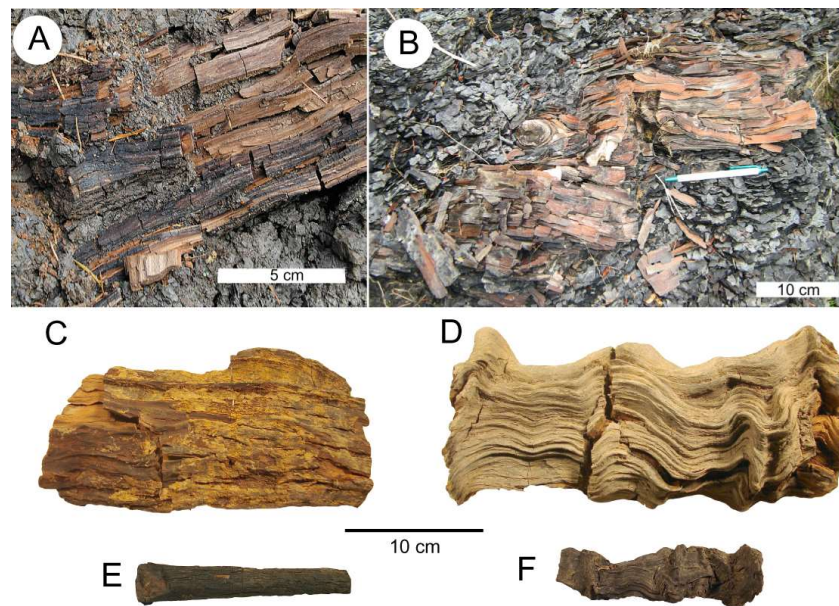


**Figure 9.** Late Miocene wood from Wilkes Formation at Salmon Creek, Washington USA. (A,B) Highly fractured wood in clay bed hat has been exposed to surface weathering. (C,D) Mummified wood typically shows compaction and distortion from burial pressures. (E,F) Some small specimens show incipient coalification.

### 3.9. Two Creek Forest, Wisconsin USA—Late Pleistocene

The Two Creeks forest bed is perhaps the most famous Quaternary deposit in the Great Lakes region in north-central USA [58]. The widespread distribution of subfossil wood was first mapped in 1970 [59], though the Two Creeks fossil forest had been described a century earlier [60], with later studies published in the 1930s [61,62]. Radiometric ages for the Two Creeks forest sediments average 13,500  $^{14}\text{C}$  years BP (Before Present), equivalent to a calendar age of 11,850 years BP [57,63], a time when spruce forest covered much of the Lake Michigan region following the recession of the great continental ice sheet. Tree-ring analyses show a duration age of the forest to have been 252 years [64] to 310 years [65]. The wood is extremely well preserved, typically showing shrinkage cracks, but few other structural defects (Figure 10). Detailed descriptions of the geologic setting and paleoenvironment can be found in references [59,66–69].

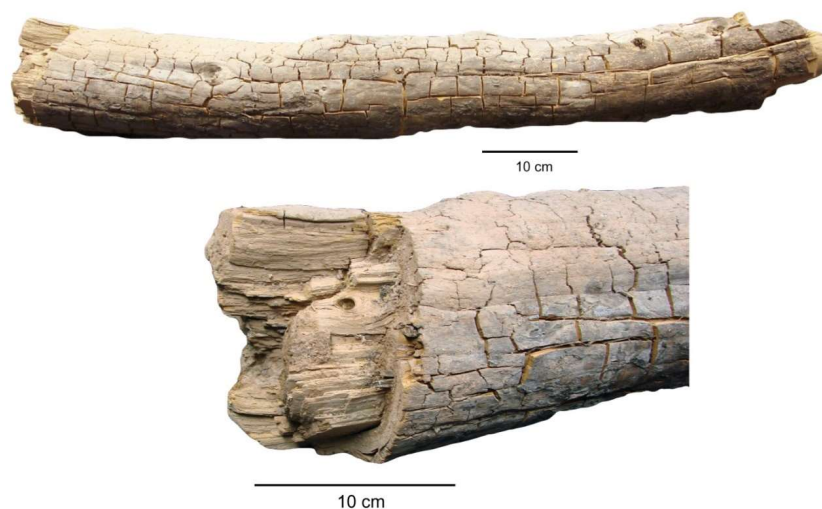


**Figure 10.** Late Pleistocene Spruce log from Two Creeks Forest, east-central Wisconsin, USA.

### 3.10. Puget Sound, Washington—Late Pleistocene

Mummified wood is abundant in Late Pleistocene interglacial deposits in the northern Puget Sound lowlands, northwest Washington, USA, where tree trunks, limbs, and small wood fragments occur in the Whidbey Formation. The region experienced multiple advances and retreats of the cordilleran ice sheet, but evidence of earlier events has largely been obscured by erosion and deposition related to the last glacial episode, the Fraser Glaciation that occurred between ~25,000–10,500 years ago. An exception occurs at Whidbey Island, where Fraser glacial deposits are underlain by prominent exposures of the much older Whidbey Formation. These sediments have ages that exceed the maximum age that can be determined by  $^{14}\text{C}$  (>40,000 years); thermoluminescence dates suggest an age of 150,000–100,000 years BP [70]. The Whidbey Formation has an exposed thickness of ~60 m at the type section; other localities expose up to 90 m of strata. In general, the strata originated as fluvial and lacustrine sediments deposited by meandering streams flowing along a coastal floodplain.

Wood samples used in this study were collected from coastal exposures at Swantown, Lagoon Point, and Double Bluffs on Whidbey Island, and Cama Beach on nearby Camano Island (Figure 11).

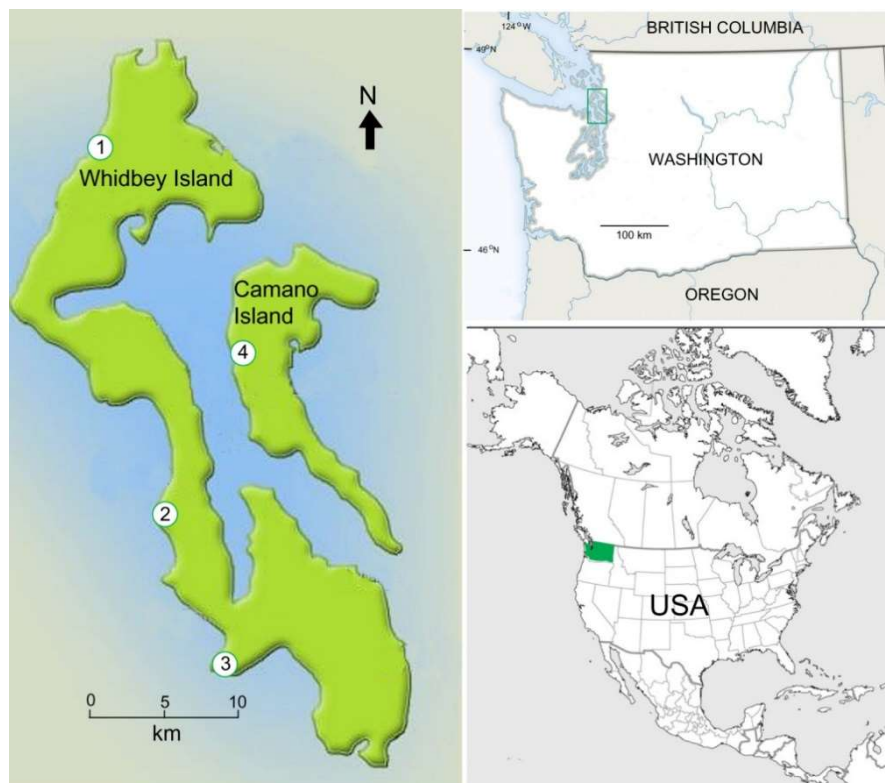


**Figure 11.** Late Pleistocene Whidbey Formation mummified wood localities, Whidbey and Camano Islands, Washington USA. (1) Swantown, (2) Lagoon Point, (3) Double Bluffs, (4) Cama Beach.

Wood occurs in two sedimentary environments. Individual logs are preserved in thick sandy beds, where they have been transported by fluvial processes. (Figure 12) Wood also occurs in beds of woody peat, ranging in form from abundant flattened stems and small twigs to large branches and rare tree trunks that accumulated in local bogs (Figure 13). Peat beds occur at multiple levels in the Whidbey Formation, interspersed with sandy fluvial deposits (Figure 14).

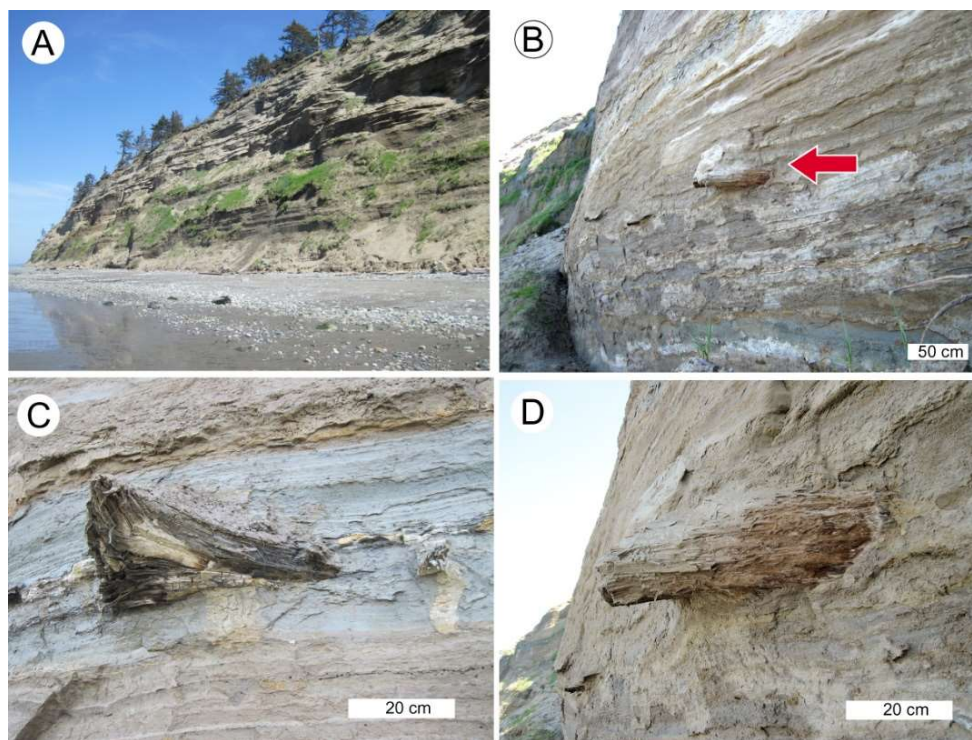


**Figure 12.** Logs in Whidbey Formation sand beds, Swantown beach, Whidbey Island, Washington USA. (A) View of Whidbey Formation strata. (B–D) Logs exposed by weathering.

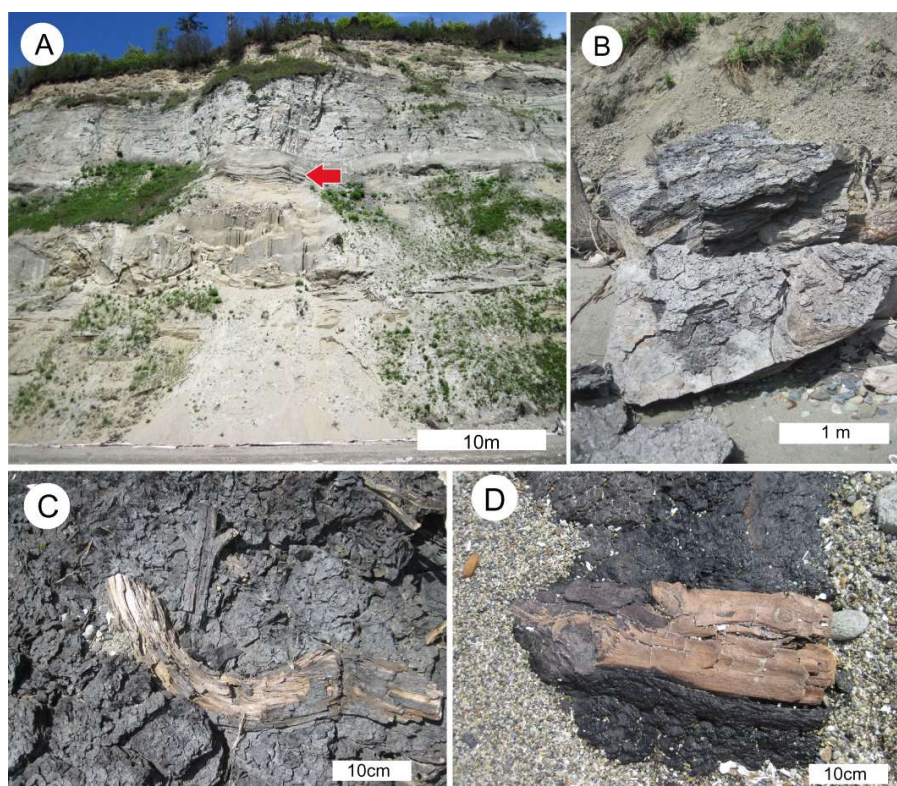


**Figure 13.** Logs in Whidbey Formation peat, Double Bluff, Whidbey Island, Washington USA. (A) Pleistocene strata at Double Bluffs. Large wood fragments occur in 2 m-thick peat beds (arrow). (B) Blocks of peat that have fallen to lie at the base of the bluff. (C,D) Wood in fallen peat blocks.

The Whidbey Formation wood is well-known to local geoscientists, but this material has received little scientific study. Poor anatomical preservation hinders taxonomic identification of the wood, but the forest that produced it is known from pollen obtained from Whidbey Formation peat beds at the Double Bluffs type locality (Figure 14) [71,72]. *Pinus contorta* (Lodgepole Pine), *Tsuga heterophylla* (Western Hemlock), and *Pseudotsuga menziesii* (Douglas Fir) are abundant elements in the palynoflora. Pollen analysis from the main wood-bearing peat bed in the Whidbey Formation type section contains the above-mentioned conifers as the most abundant taxa, but small amounts of *Juniperus* (Juniper), *Abies* (Balsam Fir), and *Betula* (Birch) are present. A thin peat bed ~20 m higher in the stratigraphic section is dominated by *Alnus* (Alder) [72]. The pollen flora indicates that during the Whidbey Formation interglacial period the region was inhabited by boreal conifer forest that closely resembles the modern flora.

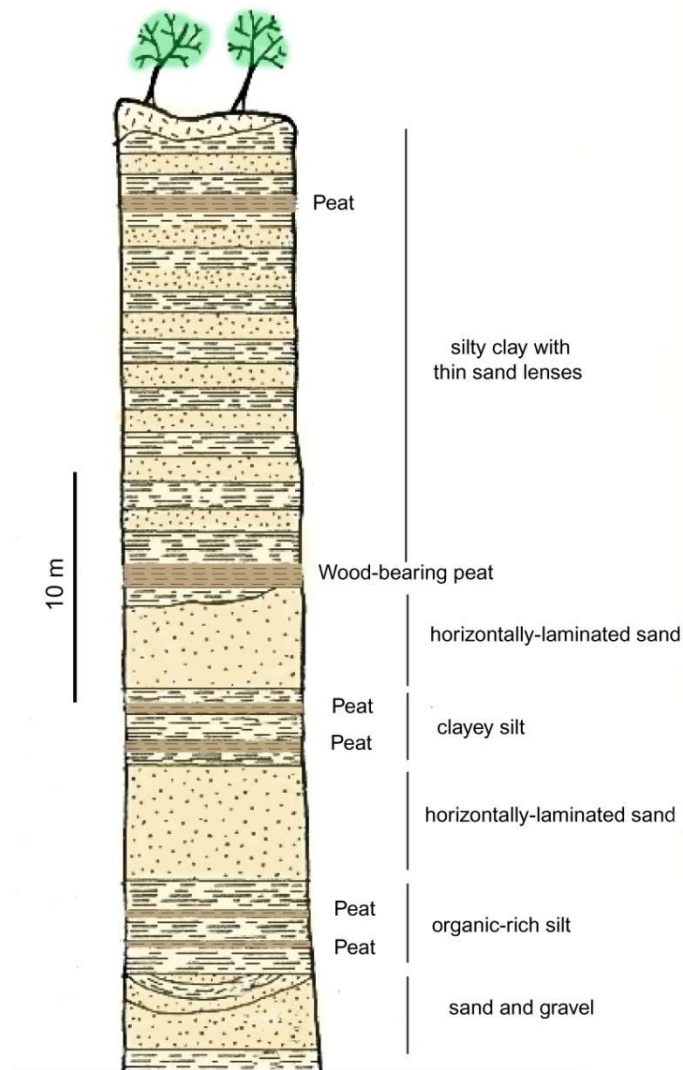


**Figure 14.** Stratigraphic section of late Pleistocene Whidbey Formation of interglacial sediment at Double Bluff, Whidbey Island, Washington USA. Adapted from [73].

Preservation quality is variable, largely affected by compression from the weight of overlying sediments. Small twigs and stems in woody peat layers are commonly highly flattened, but larger limbs and trunks are more likely to retain three-dimensional shapes. Regardless of shape, it is rare for specimens to preserve uncompressed cells (Figures 1A and 15A–D).

Whidbey Formation wood is not visibly mineralized, the only exception being a few specimens that have thin coatings of vivianite ( $\text{Fe}^{2+}\text{Fe}^{2+}_2(\text{PO}_4)_2 \cdot 8\text{H}_2\text{O}$ ), (Figure 16).

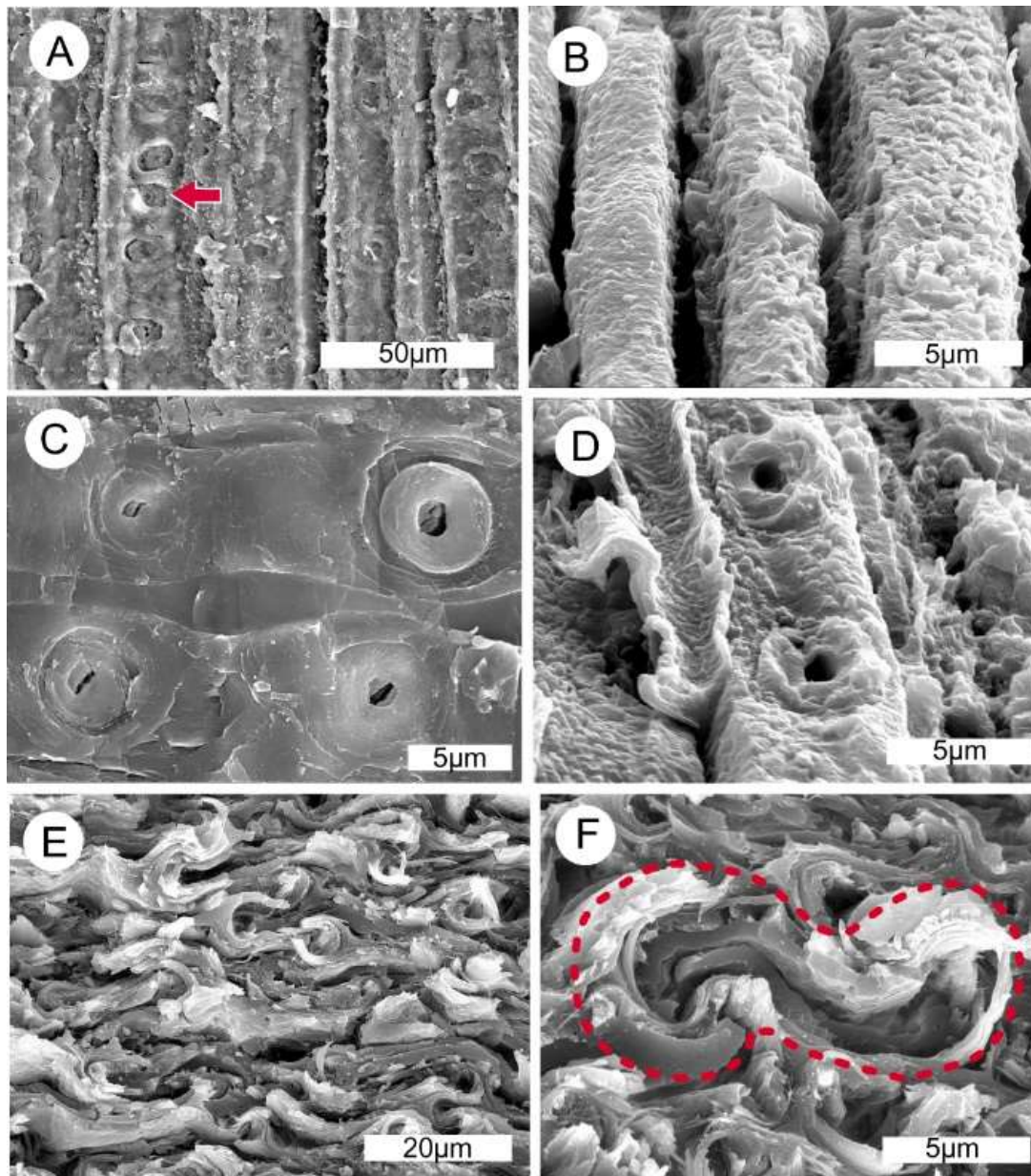


**Figure 15.** Scanning electron microscopy (SEM) photos of mummified conifer wood from the late Pleistocene Whidbey Formation, Whidbey Island, Washington USA. (A) Wood from peat bed at Double Bluff. Radial view of tracheids, showing circular pits (arrow). (B) Wood from log in sand bed at Swantown beach. Cell walls are composed of relict organic matter, but anatomical details are mostly obliterated. (C) Pits in ray cells of wood from Double Bluff peat, showing excellent preservation. (D) Radial view of wood from Swantown log, showing two pits on a cell that has altered surface texture. (E) Transverse view of wood from a limb buried in peat bed at Double Bluff. Cells walls preserve original multilayered architecture, but cells are highly compressed. (F) Transverse view of the same wood at higher magnification, showing the sigmoidal shape of a single compressed tracheid.

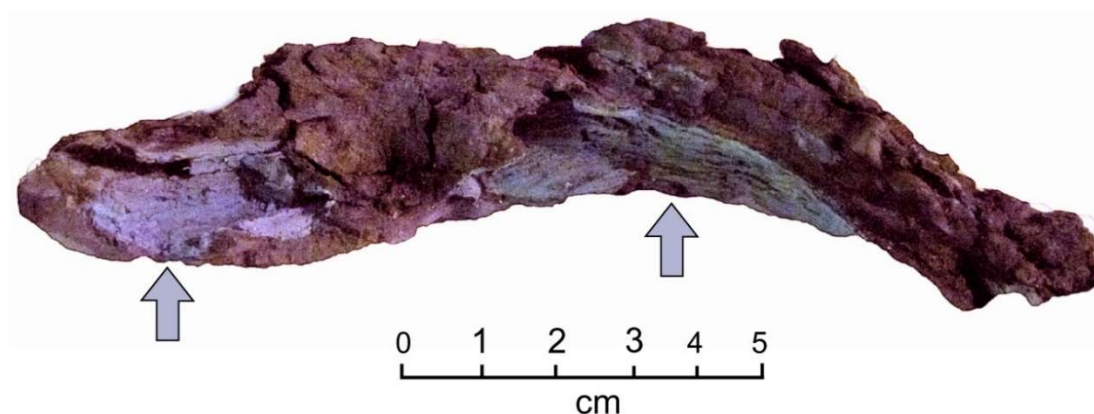


**Figure 16.** Late Pleistocene wood from northwest Washington, USA, containing coatings of blue vivianite (arrows).

### 3.11. European Locations

Mummified wood occurs at many locations in throughout the world, including numerous sites in Europe. Examples that have been reported in scientific literature include localities in Belgium [74], England [75], Austria [76], and Siberia [77,78]. Other mummified wood sites are located in Germany, Poland, Czech Republic, and The Netherlands. The following section describes some of the most spectacular occurrences at localities where efforts have been made to display evidence of fossil forests for public viewing.

### 3.12. *Ipolytarnóc Fossil Forest, Hungary—Late Miocene*

In July 2007, miners working at an open-pit coal mine at Bükkábrány, Hungary discovered 16 upright tree trunks in the sand layer just above the lignite coal seam (Figure 17A). A team of geologists and paleontologists was quickly organized to study this spectacular occurrence, the only location worldwide where large trees are preserved intending in their original forest setting [79,80]. The fossil forest is believed to have originated when rising lake waters drowned the forest during the late Miocene, with the trunks protected from decay by their deep burial in water-saturated sediment. The trees have been identified as *Glyptostroboxylon rudolphii* (Figure 17B), a taxon previously described from a site in Germany [81,82]. In 2010, a new visitor center was opened at the Ipolytarnóc Fossils Nature Reserve, where five large stumps from Bükkábrány are displayed (Figure 17C,D).

The fossil trees have commonly been described as being mummified, with the wood soft enough to cut with a razor blade after specimens were soaked in boiling water [80]. Microscopic examination and chemical analyses confirm that the wood of the buried trees is relatively pristine; levels of cellulose and phenolic compounds in wood within the underlying lignite are significantly lower, evidence of incipient gelification [83].

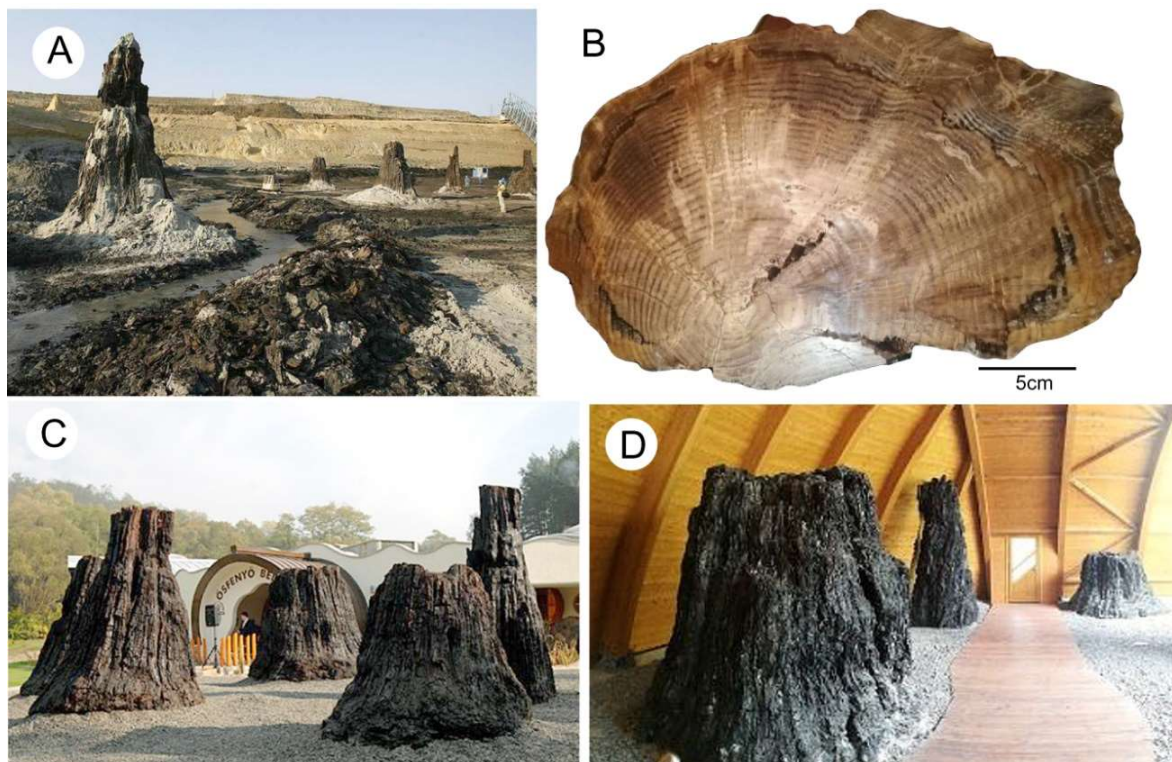


**Figure 17.** Fossil forest at Bükkábrány, northern Hungary. (A) Miocene stumps excavated in 2007 open pit lignite mine. (B) *Glyptostroboxylon rudolphii* wood. Photo by Zsigmund Atilla. (C) Large stumps that have been relocated for outdoors display at Ipolytarnóc Fossils Nature Center, opened in 2010. Photo courtesy of Tamás Elter. (D). Interior of Nature Center. Photo (D) courtesy of Sándor Kovács.

### 3.13. Dunarobba Fossil Forest, Italy—Pliocene

Discovered during clay mining in 1980, Dunarobba Fossil Forest is preserved in lacustrine sediments of the Tiberino Basin, a Plio-Pleistocene intermontane basin along the western margin of the Apennine Mountains in central Italy [84]. More than 50 upright trunks up to 2.5 m in diameter and 9 m in height are preserved in clay and fine sand sediment, representing a Pliocene conifer forest that flourished along a marshy lake shore ~3–2 Ma (Figure 18). Originally named as a member of the form genus *Taxodioxylon* [83], the dominant species is now considered to be *Glyptostrobus europaeus* based on the “whole plant” association of foliage, cones, and wood [85]. The wood is commonly described as mummified, resulting from the protection against degradation provided by the impermeable clay-rich matrix, which restricted influx of oxygenated groundwater. However, the composition of Dunarobba wood has complexities. Chemical analyses reveal that leaching has removed most polyoses and cellulose, leaving lignin as the major structural component [86,87]. Some specimens are partially mineralized with calcite, chlorapatite, chloromagnesite, and clays [88]. Permineralized wood collected from clays above the main fossil forest layer are mineralized by a combination of siderite, goethite, and ferroan calcite [89,90]. Mineral composition may vary within a single specimen, evidence that mineral precipitation was strongly influenced by localized changes in Eh and pH.

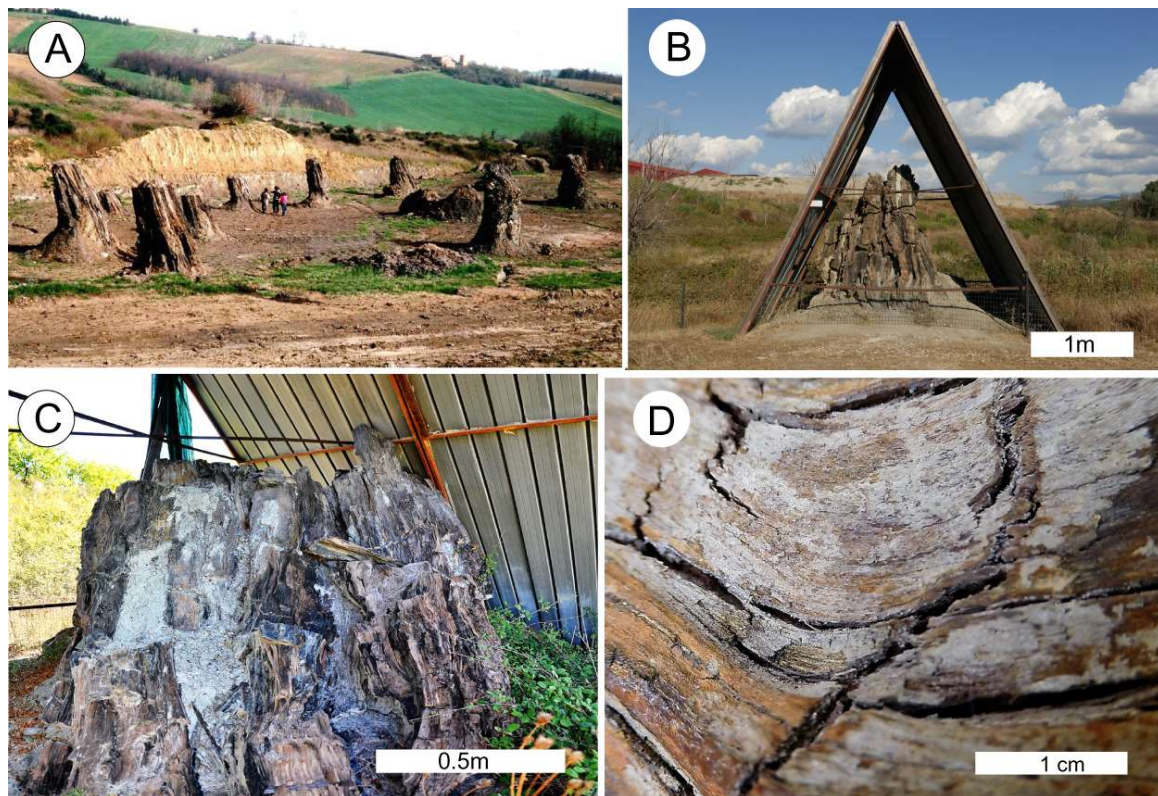


**Figure 18.** Dunarobba Fossil Forest, Umbria region of central Italy. (A) Fossil forest, circa 1995, prior to conservation. Wikipedia photo. (B) One of many outdoor stumps protected by shelters at Dunarobba Fossil Forest. Copyrighted photo from [www.alamy.com](http://www.alamy.com), used with permission. (C) View of stump within its shelter. (D) Close-up view of mummified wood showing shrinkage cracks. Photos (C,D) by Franco Bianchi, courtesy of Marta Pinzaglia.

Conservation efforts in the 1990s led to the establishment of Dunrobbia Botanic Palaeontology Centre, which includes both a small exhibition hall and a path that directs visitors to outdoor displays where upright stumps are protected by individual A-frame shelters. Preservation efforts continue in an ongoing attempt to minimize degradation caused by microbial decay and atmospheric exposure.

### 3.14. Fossano Fossil Forest, Northern Italy—Pliocene

A major Pliocene fossil forest occurs in northwestern Italy, where upright stumps are exposed along the banks of the Stura di Dimonte River near the small town of Fossano. The site is known as the Fossano Fossil Forest. The site is in proximity to the alps; the river has incised Quaternary sediments to expose Pliocene continental sediments (Figure 19). Two successive forests are represented in separate stratigraphic layers [91–93]. As in other Pliocene swamp forests in Italy, *Glyptostrobus europaeus* is the dominant tree type. The scientific significance of this newly-exposed fossil forest is sure to result in additional descriptions and interpretations in future years.

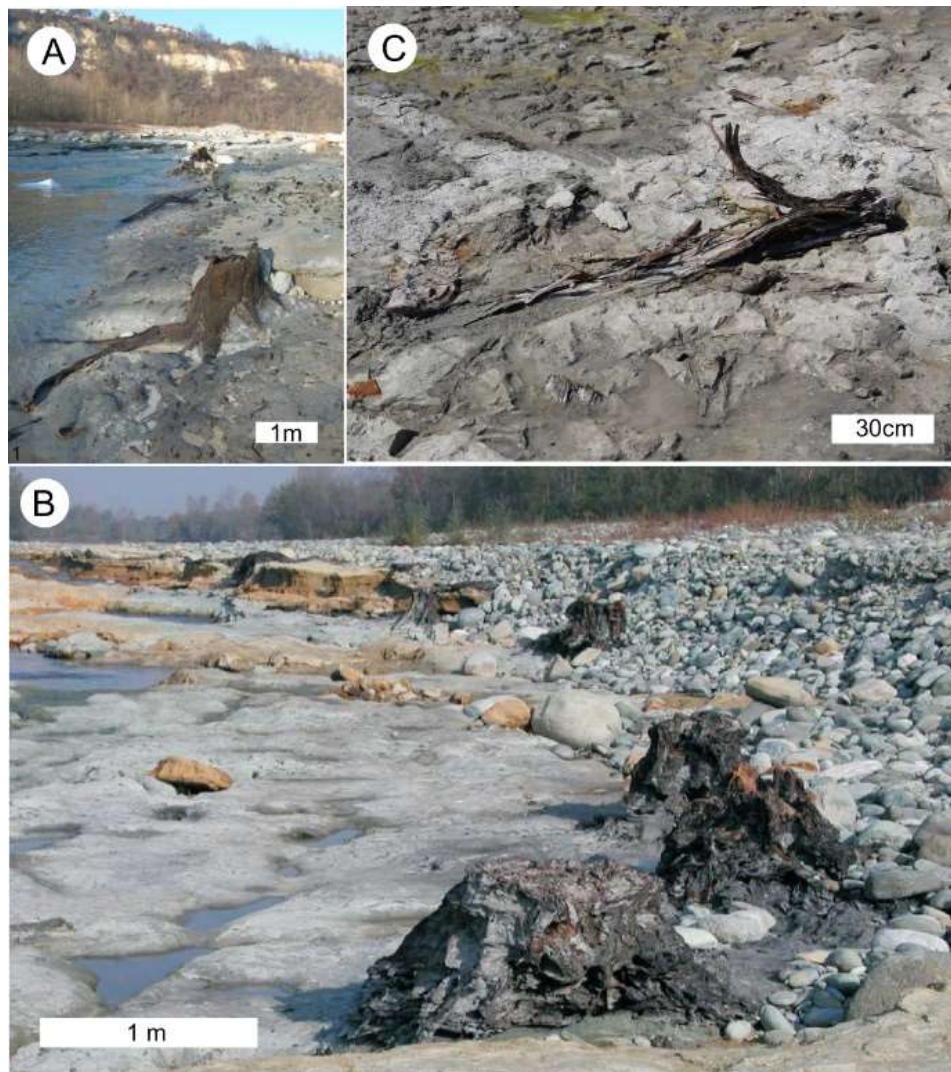


**Figure 19.** Fossano Fossil Forest, Italy. (A,B) Upright stumps of *Glyptostrobus europaeus* exposed in Pliocene sediment that forms the bed of the Stura di Dimonte River, NW Italy. (C) Wood exposed to surface conditions. Photos courtesy of Edoardo Martinetto.

### 3.15. Stura di Lanzo Fossil Forest, Northwest Italy—Pliocene

Like the Fossano Fossil Forest, the Stura de Lanzo locality is a site where mummified Pliocene tree trunks have been exposed by river erosion [94–96]. The muddy sediments that enclose large *Glyptostrobus* stumps also preserve seeds and cones, allowing “whole plant” identification [85]. The Stura di Lanzo Fossil Forest has been described in detail in a 2005 booklet [97] published in Italian by Parco la Mandria (Mandria Provincial Park). Conservation efforts at the site have included participation of teachers and young students [98,99].

### 3.16. Other Locations

In East Asia, Oligocene mummified wood occurs in the Nanning Basin of southern China. The deposit includes fossilized mollusks, fish, reptiles, and mammals as well as plants. Wood occurs as stumps and trunks in a lagerstätte that also preserves foliage and seeds [100]. Pliocene mummified wood has been described from central Japan [101].

#### 4. Charcoalified Wood

Fire has been present throughout the Earth's history, so the abundance of charred wood in the geologic record is not surprising. Production of charcoal has two primary causes: natural wildfires (Figure 20), and ignition of wood by volcanic flows or hot volcanic ash (ignimbrite) (Figure 21). Charcoal in the fossil record ranges from intact logs to tiny fragments dispersed in clastic sediments and coal. The latter form is commonly called *fusain*. Regardless of size, ancient charcoal may yield important information about Earth history.

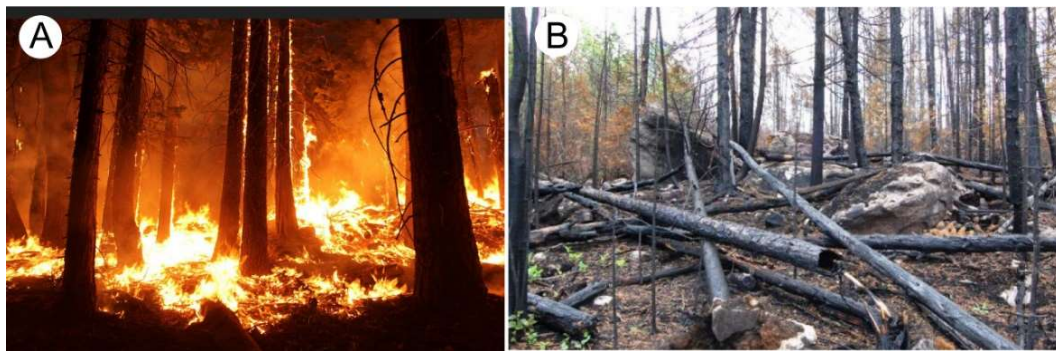


**Figure 20.** Charcoalification of wood in modern wild fires. (A) California, USA, 2015. Photo: National Atmospheric & Space Administration. (B) Charred trees after 2007 fire, Minnesota, USA. Photo courtesy of Eli Sagor.

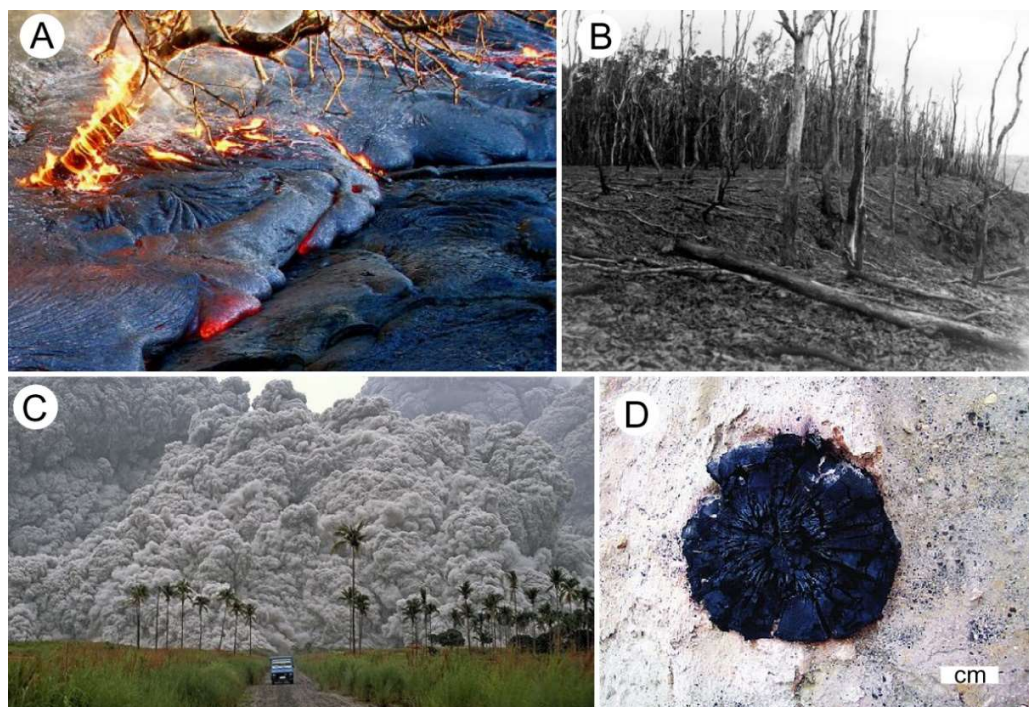


**Figure 21.** Charred wood resulting from volcanic processes. (A) Tree ignited by basalt flow from Kilauea Volcano, Hawaii, USA. Photo by Brian W. Schaller (Wikipedia). (B) Charred trees after 1959 Kilauea eruption. USGS Hawaii Volcano Observatory photo. (C) Tephra cloud engulfing palm grove, 1991 Mt. Pinatubo eruption, Philippine Islands. Photo by Alberto Garcia. (D) Recent charcoal in ignimbrite, Taupo volcanic field, New Zealand. Photo by Brent Alloway.

Much of our knowledge of ancient charcoal comes from the work of University of London professor Andrew C. Scott. His research is described in a recent book [96], and in many journal publications [102–106]. Several papers provide general overviews of fossil charcoal research [104–106].

Because charred wood typically has excellent anatomical preservation, intact charcoal specimens are well suited for taxonomic identifications. For relatively young deposits, charcoal is in an ideal material for  $^{14}\text{C}$  radiometric dating. Like other plant fossils, charcoal can be used to reconstruct paleoenvironmental conditions. On a global scale, ignition temperature of plant material is related to atmospheric oxygen levels, so the presence of charcoal can be used to trace atmospheric evolution [107].

Charring of wood by volcanic processes has been described for the Soufrière Hills Volcano, Monserrat [103], the Miocene volcanic field at Cormandel Peninsula, New Zealand [108] and Recent ignimbrite in the Taupo volcano, New Zealand [109]. In the latter example, charring temperatures estimated from optical reflectance ranged from 267 °C to 414 °C, generally decreasing at distances away from the volcanic vent. At Montserrat, charring temperatures are estimated to mainly be in the range of 200 °C–340 °C, with a possible maximum of ~450 °C [104]. In volcanic environments, it is common for tree trunks to be completely charred, though some specimens are less charred in interior regions.

#### 4.1. Evidence of Ancient Wildfires

Fossil evidence of wildfires primarily comes from charcoal. The oldest known charcoal comes from the Silurian [110]. However, wildfires did not become prominent until the appearance of forests in the Middle Devonian [111,112]. By the Carboniferous, high-biomass forests were episodically swept by fires, ultimately producing coal that contains as much as 20% charcoal by volume [99]. The occurrence of fire is related to atmospheric oxygen levels, which determine the ignition temperature of organic materials. Atmospheric oxygen levels during Phanerozoic time was estimated from the organic carbon and sulfur content of clastic sediments [113–115], but the usefulness of fossil charcoal for making more precise evaluations was quickly recognized. A minimum oxygen concentration of 13% is required for wildfires; oxygen levels above 35% would reduce ignition temperatures to a point where sustained forest growth would be prohibited [114]. Atmospheric oxygen concentrations are estimated to have been above 26% throughout the Carboniferous and Permian periods, declining abruptly near the time of the Permian-Triassic mass extinction, fluctuating during the Triassic and Jurassic, and declining beginning in the mid Cretaceous to reach the present-day value of ~21% [116–118]. Dispersed charcoal is commonly preserved in clastic sediments, but also occurs in lignite coal [119].

#### 4.2. Anatomical Evidence

Dispersed charcoal fragments are useful for tracing wildfire history, but macroscopic specimens are valuable for taxonomic purposes. Light microscopy can be used, but SEM images are richer in detail. Although most research has been done on charred wood, vascular plants (e.g., ferns) may also be represented as fossil charcoal [120]. In higher plants, charred tissues become black and brittle, with a silky sheen. Because charcoal results from heating, compression forces are limited to minor shrinkage effects, so wood retains its 3-dimensional structure. The reflectance of the charcoal can be used to estimate charring temperature [105, 107]. The most significant structural change is the fusing of the cell walls into a single homogeneous layer, obliterating the original multilayered architecture. Experimental studies show that cell wall homogenization may occur when modern conifer wood is heated for one hour at 350 °C [105,116]. In other aspects, anatomical preservation may be excellent (Figure 22).

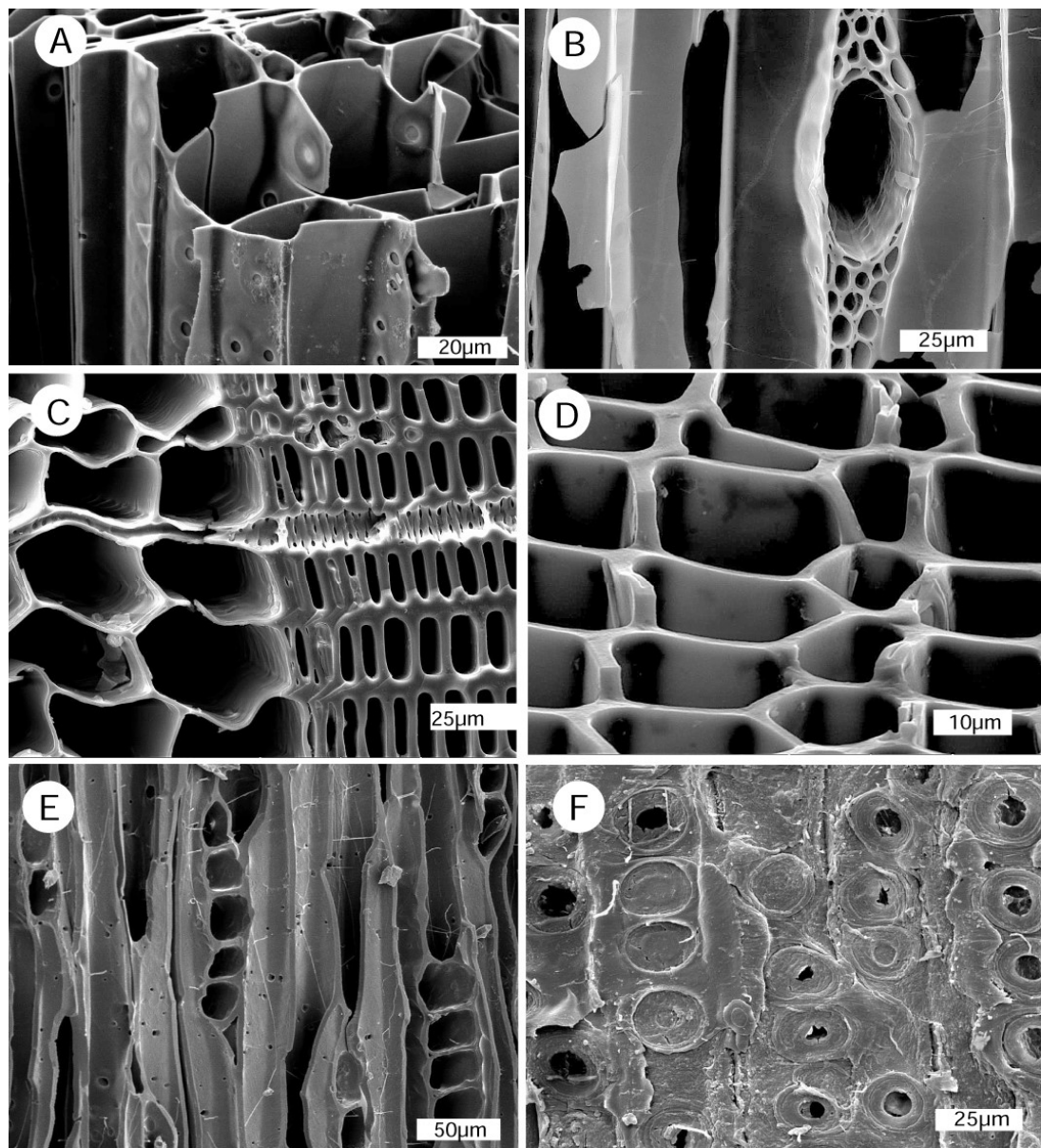


**Figure 22.** Modern charred wood from Whatcom County, Washington USA. (A) *Thuja plicata* (Red Cedar), wildfire wood; (B–D) *Acer macrophyllum* (Bigleaf Maple), camp fire wood. (B) Tangential view, showing cross-section of a ray with a conspicuous resin canal. Adjacent tracheid cell walls show brittle fracture. (C), Transverse view showing earlywood (large cells) and latewood (small cells). (E,F) Charred conifer wood from an excavated landfill. (E) Tangential view, showing cross-section view of ray cells. (F) Radial view showing well-preserved bordered pits.

A few occurrences have been reported where partially-charred wood has become silicified [108,121]. A previously unreported occurrence is represented by a single specimen from the Miocene Columbia Plateau basalts of central Washington, USA (Figure 23A). Although the opal mines at Virgin Valley are famous for silicified wood, a few samples show charring, presumably from pyroclastic flows that affected forests bordering the ancient caldera. These examples provide evidence that charred wood is not susceptible to silicification, probably because the pyrolyzed tissues are not capable of acting as organic templating matrices for the precipitation of silica. However, uncharred interior regions and empty cell lumen may be sites for silica precipitation (Figure 23B,C).

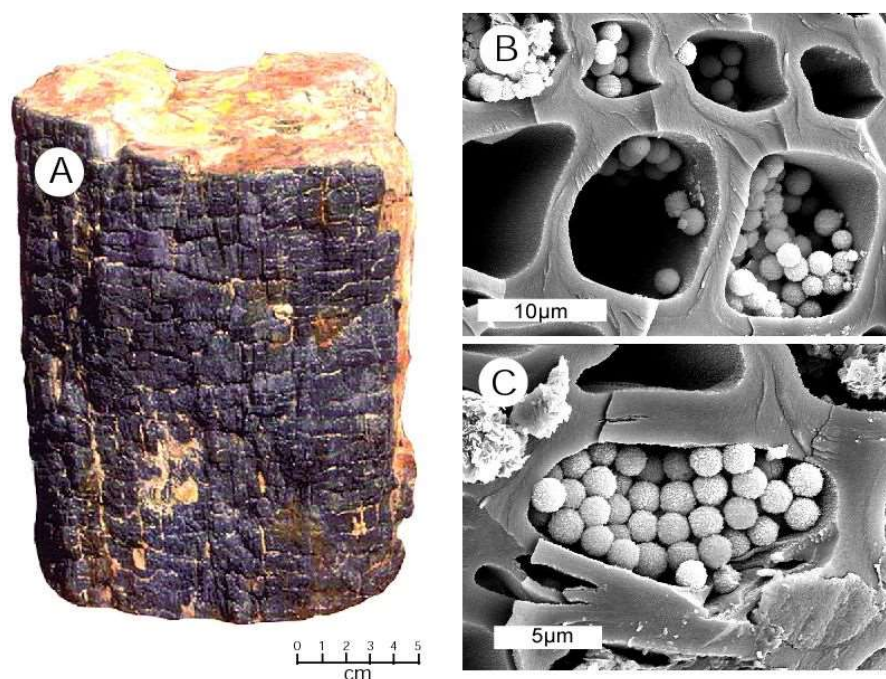


**Figure 23.** Silicification of charred wood. (A) Miocene wood from Columbia River Basalt Group, central Washington, USA. Exterior charred layer surrounds silicified interior wood. (B,C) Miocene wood from Royal Peacock Opal Mine, Virgin Valley, Nevada USA, showing homogenization of charred cell walls. Cell lumen contain lepispheres of opal-CT.

## 5. Coalified Wood

Mummified wood retains a high proportion of the original cellulosic constituents, in contrast to coalified wood, where loss of cellulose and hemicellulose results in relative enrichment of lignin [73]. During coalification, wood and other plant remains are transformed to peat as a result of humification and gelification, which are biochemical processes. Humification involves the decomposition of original organic constituents to produce dark brown organic polymers. Because these polymers are resistant to microbial attack, peat is a relatively stable material. The amorphous nature of these organic alteration products causes plant tissues to lose their original architecture, producing a gelatinous texture. The conversion of peat to coal is a metamorphic process, where organic compounds are altered as a result of heat and pressure, leading to an increase in carbon content and decreases in oxygen and hydrogen. These reactions involve dehydration, bituminization, and graphitization, and they can be divided into four stages: peat is successively changed into lignite, subbituminous coal, bituminous, and anthracite [122]. Coal is composed of three microscopically-recognizable groups of organic constituents that are known as *macerals*. Derived from cellular tissues, vitrinite is the most abundant and most homogeneous maceral, the main contributor to the shiny black appearance of coal. U.S. Coals typically contain as much as 80 wt % vitrinite [123]. Liptinite (also called exinite) originates from spores, pollen, resins, lipids, waxes, algae, and bacterial proteins. Inertinite is derived from oxidation. Coalified wood is most commonly found in the lowest-rank coals, lignite and subbituminous, where the macroscopic organic remains may be preserved. Preservation of wood in lignite (brown coal) is very common (e.g., [124–126]). However, cellular tissues in a mineralized Permian tree fern have been observed to consist of anthracite [127]. Conversion of original tissue to vitrinite involves the diagenetic alteration of lignocelluloses. In general, both hemi-cellulose and cellulose are greatly reduced or destroyed, and lignin-based components are selectively enriched. [127,128]. Key drivers of vitrinite formation are removal of cellulosic materials followed by physical compression. The result is that cellular anatomy is likely to be destroyed, producing logs and limbs that retain their original form, but often with significant flattening. Coalified wood typically has a vitreous or semi-vitreous luster, brittle with

conchoidal fracture (Figure 24). Microscopically, coalified wood cells are typically comminuted and homogenized (Figure 25).

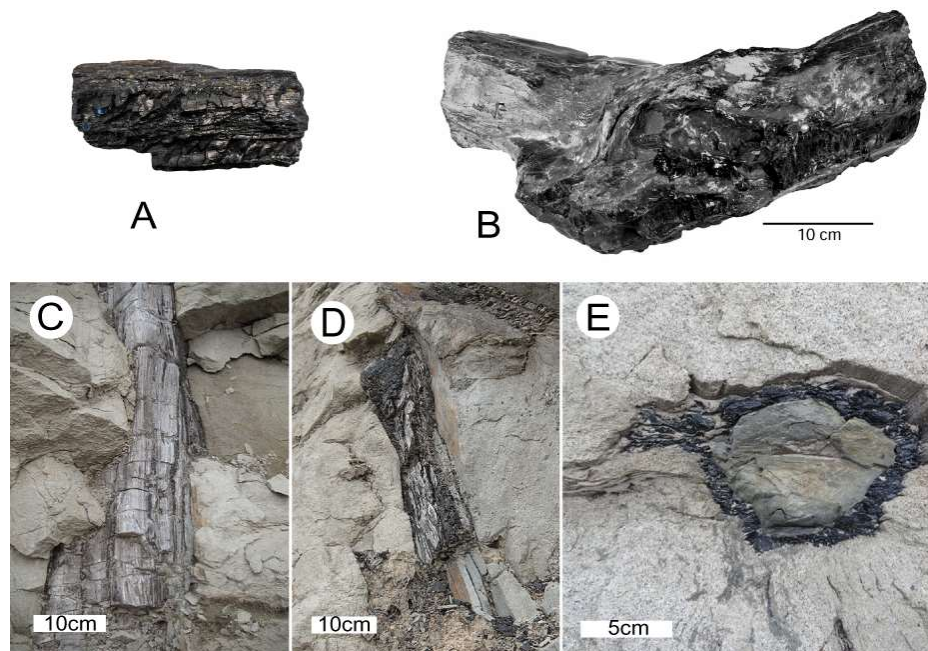


**Figure 24.** Coalified wood. (A) Coalified wood fragment from Eocene Colestin Formation, Siskiyou Pass, Oregon USA [129]. (B–E) Eocene Chuckanut Formation, Whatcom County, WA USA. (B) coalified log, Bellingham Coal Mine. (C–E) Driftwood logs in fluvial sandstone at Lookout Mountain. Outer bark layer has been coalified, inner wood has decayed and been replaced by sandstone.

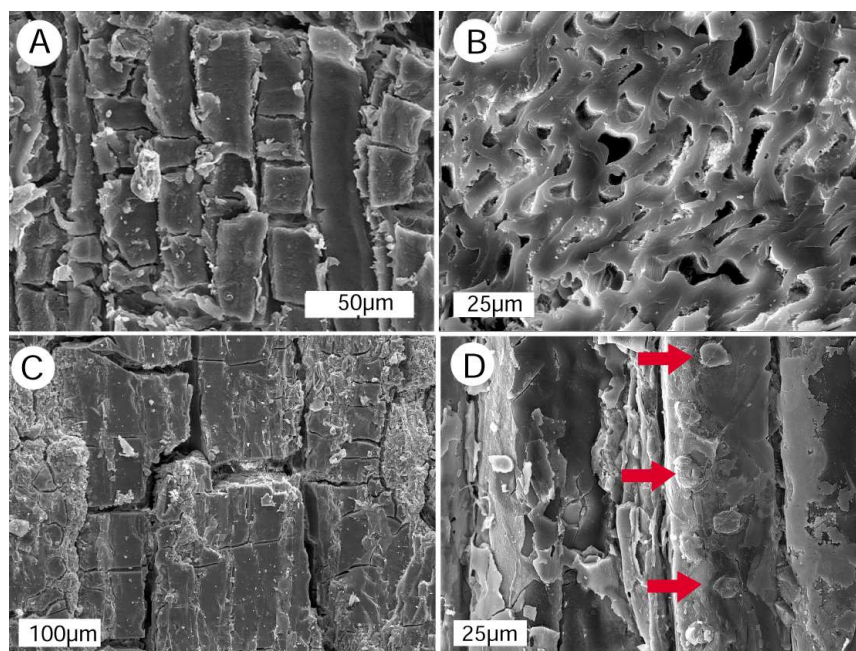


**Figure 25.** SEM images of coalified wood. (A,B) Late Pleistocene Whidbey Formation, Swantown beach, Washington, USA. (A) longitudinal views showing brittle fracture of tracheids, (B) transverse view showing homogenized cell walls, (C,D) Oligocene Colestin Formation, Siskiyou Pass, Oregon USA. Arrows show relict pits.

### 5.1. Coexistence of Mummified and Coalified Wood

Fossil forests in the Whidbey Formation and Wilkes Formation in Washington, USA and Axel Heiberg and Ellesmere Islands in the Canadian Arctic primarily contain both mummified wood, but coalified wood is also present. The occurrence of both mummified and coalified wood in a single formation, sometimes within a single stratum, is evidence that conditions of preservation are subject to localized variation. Because the alteration of original organic matter to bituminous products involves a reduction in volume, coalified specimens are typically compressed. At the Eocene fossil forest at Axel Heiberg Island, Canadian Arctic, coalified wood is estimated to have been compressed at a ratio of ~6:1 relative to the original wood [44].

### 5.2. Accessory Minerals in Mummified and Coalified Wood

The original preface of this paper is a description of fossil woods that are composed of original organic matter or its alteration products. However, nature seldom obeys simple rules, and it is not unusual for non-silicified wood to contain small amounts of inorganic minerals that were introduced during diagenesis. This phenomenon usually involves the precipitation of microcrystalline minerals within empty cell lumen. Figure 26 shows Eocene wood from Yuba River, California. Cell walls have been fused to produce a homogenous carbon layer, suggestive of charring. Individual cell lumen contain a variety of different diagenetic minerals, including apatite, pyrite, and gypsum. Siderite ( $\text{FeCO}_3$ ) has previously been reported as a major component of Neogene coalified wood in Alaska, USA [130]. Cretaceous wood from New Mexico, USA, has been reported to contain quartz, apatite, and calcite [131]; small amounts of pyrite, siderite, and clay minerals occur in coalified Miocene tree stumps at the Bilna Mine, Czech Republic [132].

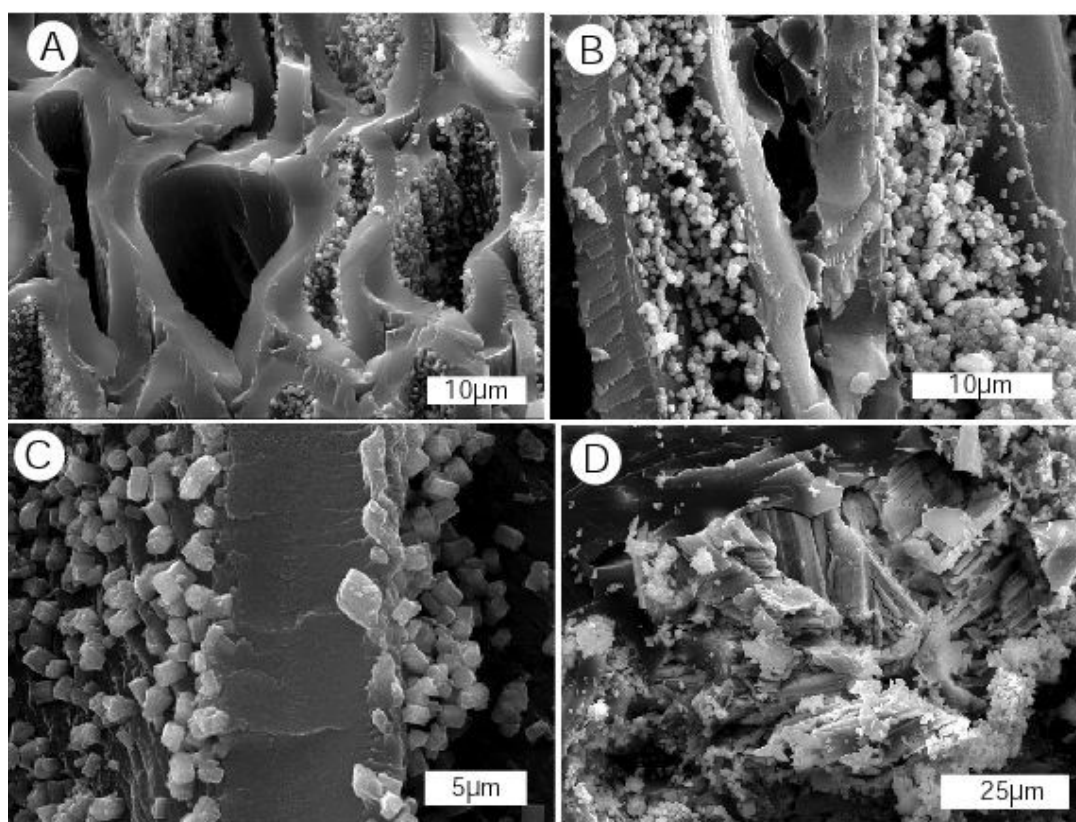
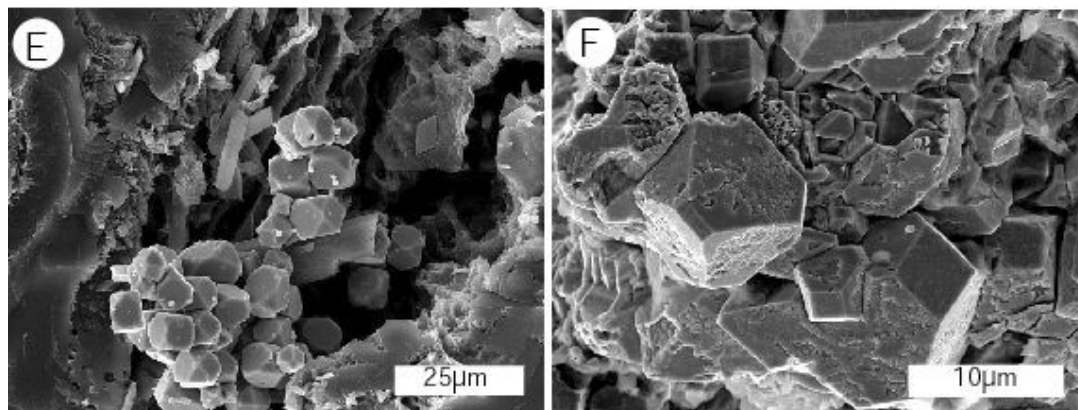


Figure 26. Cont.



**Figure 26.** SEM images of accessory minerals in Eocene charred wood from Yuba River, California, USA. (A) Transverse view shows homogenized cell walls, with diagenetic apatite crystals dispersed over inner surfaces of some cells. (B) Longitudinal view of two tracheids, showing abundant apatite. Apatite does not occur in intracellular spaces. (C) Apatite crystals are attached to surfaces of cell wall separating two adjacent tracheids. (D) Tabular gypsum crystals occur on outer surfaces of the wood, apparently representing a very late stage precipitation event. (E,F) Pyrite crystals are present in some cell lumen. The presence of gypsum ( $\text{CaSO}_4 \cdot 2\text{H}_2\text{O}$ ) and pyrite ( $\text{FeS}_2$ ) are evidence of the availability of dissolved sulfur in pore fluids during diagenesis.

**Funding:** This research received no external funding.

**Acknowledgments:** The author thanks the following people for generously providing photographs: Brent Alloway, Franco Bianchi, Tamás Elter, Alberto Garcia, David Greenwood, Hope Jahren, William Hagopian, Benjamin Hook, Sándor Kovács, Edoardo Martinetto, Mark Orsen, Marta Pinzagli, Natalia Rybcynski, Eli Sagor, Brian Schaller, Chris Williams. Fossil wood specimens were contributed by David Lawler, Jim Meissner, and Alex Wolfe. Charles Wampler and Dan Carnevale provided technical support for the SEM used in this research.

**Conflicts of Interest:** The author declares no conflicts of interest.

## References

1. Rocky Mountain Tree Ring Research. Available online: [www.rmtrr.org/oldlist.htm](http://www.rmtrr.org/oldlist.htm) (accessed on 18 May 2018).
2. Grant, M.C. The trembling giant. Available online: [www.discovermagazine.com/1993/oct/thetremblinggiant285](http://www.discovermagazine.com/1993/oct/thetremblinggiant285) (accessed on 18 May 2018).
3. Mustoe, G.E. Wood petrification: A new view of permineralization and replacement. *Geosciences* **2017**, *7*, 1–17. [[CrossRef](#)]
4. Mustoe, G.E. Mineralogy of non-silicified wood. *Geosciences* **2018**, *8*, 1–32. [[CrossRef](#)]
5. Akahane, H.; Furuno, T.; Miyajima, H.; Yoshikawa, T.; Yamamoto, S. Rapid wood silicification in hot spring water: An explanation of silicification of wood during the Earth's history. *Sediment. Geol.* **2004**, *169*, 219–228. [[CrossRef](#)]
6. Hellawell, J.; Ballhaus, C.; Gee, C.T.; Mustoe, G.E.; Nagel, T.J.; Wirth, R.; Rethemeyer, J.; Tomaschek, F.; Geisler, T.; Greef, K.; Mansfeldt, T. Incipient silicification of recent conifer wood at a Yellowstone hot spring. *Geochim. Cosmochim. Acta* **2014**, *149*, 79–87. [[CrossRef](#)]
7. Channing, A.; Edwards, D. Experimental taphonomy: Silicification of plants in Yellowstone hot-spring environments. *Trans. R. Soc. Edinb.* **2003**, *94*, 503–521. [[CrossRef](#)]
8. Ericksen, K.E.L.; Blanchette, R.A.; Ander, P. *Microbial and Enzymatic Degradation of Wood and Wood Components*; Springer Verlag: Berlin, Germany, 1990; 407p.
9. Passialis, C.N. Physico-chemical characteristic of waterlogged archaeological wood. *Holzforschung* **1997**, *51*, 111–113. [[CrossRef](#)]
10. Fengel, D. Ageing and fossilization of wood and its components. *Wood Sci. Technol.* **1991**, *25*, 153–177. [[CrossRef](#)]

11. Kim, Y.S.; Sing, A. Micromorphological characteristics of wood biodegradation in wet environments: A review. *IAWA J.* **2000**, *21*, 135–155. [[CrossRef](#)]
12. Klusek, M.; Pawelczyk, S. Stable carbon isotope analysis of subfossil wood from Australian Alps. *Geochronometrica* **2014**, *41*, 400–408.
13. Barghoorn, E. Degradation of plant tissues in organic sediments. *J. Sediment. Petrolog.* **1952**, *2*, 34–41.
14. Blanchette, R.A.; Cease, K.R.; Abad, A.R.; Burnes, T.A. Ultrastructural characterization of wood from Tertiary fossil forests in the Canadian Arctic. *Can. J. Bot.* **1991**, *69*, 560–568. [[CrossRef](#)]
15. Jahren, A.H.; Sternberg, L.S.L. Humidity evidence for the middle Eocene Arctic rain forest. *Geology* **2003**, *31*, 463–466. [[CrossRef](#)]
16. Richter, S.L.; Johnson, A.H.; Dranoff, M.M.; LePage, B.A.; Williams, C.J. Oxygen isotope ratios in fossil wood cellulose: Isotopic composition of Eocene-to-Holocene-aged cellulose. *Geochim. Cosmochim. Acta* **2008**, *72*, 2744–2753. [[CrossRef](#)]
17. Jahren, A.H.; Sternberg, L.S.L. Annual patterns within tree rings of the Arctic middle Eocene. (ca. 45 Ma): Isotopic evidence of precipitation, relative humidity, and deciduousness. *Geology* **2008**, *36*, 99–102. [[CrossRef](#)]
18. Eberle, J.J.; Greenwood, D.R. Life at the top of the greenhouse Eocene world—A review of the Eocene flora and vertebrate fauna from Canada's High Arctic. *Geol. Soc. Am. Bull.* **2012**, *124*, 3–23. [[CrossRef](#)]
19. Taggart, R.E.; Cross, A.T. Global greenhouse to icehouse and back again: The origin and future of the Boreal Forest biome. *Glob. Planet. Chang.* **2009**, *65*, 115–121. [[CrossRef](#)]
20. Greely, A.W. Report of Sergeant D.L. Brainard on a petrified forests discovered May 20, 1883, near Cape Baird 81°30' N, 64° W. In *Three Years of Arctic Service, Volume 2, Appendix 14*; Charles Scribner's Sons: New York City, NY, USA, 1886; pp. 419–420.
21. Francis, J.E. A 50-million year old fossil forest from Strathcona Fjord, Ellesmere Island, Arctic Canada. *Arctic* **1988**, *41*, 314–318. [[CrossRef](#)]
22. Williams, C.J.; Johnson, A.H.; LePage, B.; Vann, D.R.; Sweda, T. Reconstruction of Tertiary forests. II. Structure, biomass, and productivity of the Eocene floodplain forests in the Canadian Arctic. *Paleobiology* **2003**, *29*, 271–292. [[CrossRef](#)]
23. Dolezych, M.; Estrada, S. A fossil wood of *Taxodium vandenburghi* in Palaeogene sediment of Ellesmere Island (Nunavut, Canada). *Z. Dt. Ges. Geowiss.* **2012**, *163*, 283–292.
24. Mitchell, W.T.; Rybczynski, N.; Schröder-Adama, C.; Hamilton, P.N.; Smith, R.; Douglas, M. Stratigraphic and paleoenvironmental reconstruction of a mid-Pliocene fossil site in the High Arctic (Ellesmere Island, Nunavut): Evidence of an ancient peatland with beaver activity. *Arctic* **2016**, *68*, 185–204. [[CrossRef](#)]
25. Davies, N.S.; Gosse, J.C.; Rybczynski, N. Cross-bedded woody debris from a Pliocene forest river stem in the High Arctic Beaufort Formation, Meighen Island, Canada. *J. Sediment. Res.* **2014**, *84*, 19–25. [[CrossRef](#)]
26. Jahren, A.H. The Arctic forest of the middle Eocene. *Annu. Rev. Earth Planet. Sci.* **2007**, *35*, 509–540. [[CrossRef](#)]
27. Basinger, J.F.; McIver, E.E.; LePage, B.A. The fossil forests of Axel Heiberg Island. *Musk-Ox* **1988**, *36*, 50–55.
28. Basinger, J.F. The fossil forests of the Buchanan Lake Formation (early Tertiary), Axel Heiberg Island, Canadian Arctic Archipelago: Preliminary floristics and paleoclimate. In *Tertiary Fossil Forests of the Geodetic Hills, Axel Heiberg Island, Arctic Archipelago*; Christie, R.L., McMillan, N.J., Eds.; Geological Survey of Canada Bulletin 403: Ottawa, ON, Canada, 1991; pp. 39–65.
29. Francis, J.E. Polar fossil forests. *Geol. Today* **1990**, *6*, 92–95. [[CrossRef](#)]
30. Francis, J.E. The dynamics of polar fossil forests: Tertiary fossil forests of Axel Heiberg Island, Canadian Arctic Archipelago. In *Tertiary Fossil Forests of the Geodetic Hills, Axel Heiberg Island, Arctic Archipelago*; Christie, R.L., McMillan, N.J., Eds.; Geological Survey of Canada: Ottawa, ON, Canada, 1991; pp. 29–38.
31. Christie, R.L.; McMillan, N.J. *Tertiary Fossil Forests of the Geodetic Hills, Axel Heiberg Island, Arctic Archipelago*; Geological Survey of Canada Bull. 403: Ottawa, ON, Canada, 1991; pp. 1–227.
32. Greenwood, D.R.; Basinger, J.F. Stratigraphy and floristics of peat-coal layers in Eocene swamp forests from Axel Heiberg Island, Canadian Arctic Archipelago. *Can. J. Earth Sci.* **1993**, *30*, 1914–1923. [[CrossRef](#)]
33. Greenwood, D.R.; Basinger, J.F. The paleoecology of high-latitude Eocene swamp forests from Axel Heiberg Island, Canadian High Arctic. *Rev. Palaeobot. Palynol.* **1994**, *81*, 83–97. [[CrossRef](#)]

34. Irving, E.; Wynne, P.J. The paleoaltitude of the Eocene fossil forests of the Geodetic Hills, Axel Heiberg Island, Arctic Archipelago. In *Tertiary Fossil Forests of the Geodetic Hills, Axel Heiberg Island, Arctic Archipelago*; Christie, R.L., McMillan, N.J., Eds.; Geological Survey of Canada Bull. 403: Ottawa, ON, Canada, 1991; pp. 209–211.
35. Basinger, J.F.; Greenwood, D.G.; Sweda, T. Early Tertiary vegetation of Arctic Canada and its relevance to paleoclimatic interpretation. In *Cenozoic Plants and Climates of the High Arctic v. 27*; Boulter, M.C., Fisher, H.C., Eds.; NATO ASI Series I; Springer-Verlag: Berlin, Germany, 1994; pp. 175–198.
36. Kumagai, H.; Sweda, T.; Hayashi, K.; Kojima, S.; Basinger, J.F.; Shibuya, M.; Fukao, Y. Growth ring analysis of early Tertiary conifer woods from the Canadian High Arctic and its paleoclimatic interpretation. *Palaeogeogr. Palaeoclimatol. Palaeoecol.* **1995**, *116*, 247–262. [[CrossRef](#)]
37. Jahren, A.H.; Byrne, M.C.; Graham, H.V.; Sternberg, L.S.L.; Summons, R.E. The environmental water of the middle Eocene Arctic: Evidence from  $\delta D$ ,  $\delta^{18}O$  and  $\delta^{13}C$  within specific compounds. *Palaeogeogr. Palaeoclimatol. Palaeoecol.* **2009**, *271*, 96–103. [[CrossRef](#)]
38. Jahren, A.H.; LePage, B.A.; Werts, S.P. Methanogenesis in Eocene Arctic soils inferred from (EY13C of tree fossil carbonates. *Palaeogeogr. Palaeoclimatol. Palaeoecol.* **2004**, *214*, 347–358. [[CrossRef](#)]
39. Williams, C.J.; Mendell, E.K.; Murphy, J.; Court, W.M.; Johnson, A.H.; Richter, S.L. Paleoenvironmental reconstruction of a Miocene forest from the western Canadian Arctic. *Palaeogeogr. Palaeoclimatol. Palaeoecol.* **2008**, *261*, 160–176. [[CrossRef](#)]
40. LePage, B.A.; Basinger, J.F. Early Tertiary *Larix* from the Buchanan Lake Formation, Canadian Arctic, and a consideration of the phytogeography of the genus. *Geol. Surv. Can. Bull.* **1991**, *403*, 67–82.
41. LePage, B.A.; Basinger, J.F. A new species of *Larix* (Pinaceae) from the early Tertiary of Axel Heiberg Island, Arctic Canada. *Rev. Palaeobot. Palynol.* **1991**, *70*, 89–111. [[CrossRef](#)]
42. Harrington, G.J.; Eberle, J.; LePage, B.A.; Dawson, M.; Hutchison, J.H. Arctic plant diversity in the Early Eocene greenhouse. *Proc. R. Soc. B Biol. Sci.* **2010**, *279*, 1515–1521. [[CrossRef](#)] [[PubMed](#)]
43. Kaelin, P.E.; Hugget, W.H.; Anderson, K.B. Comparison of vitrified and unvitrified Eocene woody tissue by TMAH thermochemolysis—Implications for the early stages of formation of vitrinite. *Geochem. Trans.* **2006**, *7*, 1–12. [[CrossRef](#)] [[PubMed](#)]
44. Fyles, J.G.; Hills, L.V.; Matthews, J.V., Jr.; Barendregt, R.; Baker, J.; Irving, E.; Jette, H. Ballast Brook and Beaufort Formations (Late Tertiary) on northern Banks Island, Arctic Canada. *Quat. Int.* **1994**, *22/23*, 141–171. [[CrossRef](#)]
45. Mendell, E. Using fossil trees to estimate paleoclimate of Banks Island, Arctic Canada and the effects of modern climate change on the Arctic. In Proceedings of the 19th Annual Keck Symposium in Geology, Amherst, MA, USA, 20–23 April 2006; pp. 14–19. Available online: <http://keck.wooster.edu/publications> (accessed on 18 April 2018).
46. Hills, L.V. *Beaufort Formation, Northwestern Banks Island, District of Franklin*; Paper 69-1A; Geological Survey of Canada Bull. 403: Ottawa, ON, Canada, 1969; pp. 204–207.
47. Hills, L.V. The stratigraphy, sedimentology, and paleobotany of the Beaufort Formation, Arctic Archipelago, Canada. In Proceedings of the Workshop on Circum-Arctic Late Tertiary/Early Pleistocene Stratigraphy and Environments, Denver, CO, USA, 15–17 October 1987; pp. 1–3.
48. Hills, L.V.; Ogilvie, R.T. *Picea banksii* n. sp., Beaufort Formation (Tertiary), northwestern Banks Island, Arctic Canada. *Can. J. Bot.* **1970**, *48*, 457–464. [[CrossRef](#)]
49. Hills, L.V.; Klován, J.E.; Sweet, A.R. *Juglans eocinera* n. sp., Beaufort Formation (Tertiary), southwestern Banks Island, Arctic Canada. *Can. J. Bot.* **1974**, *52*, 65–90. [[CrossRef](#)]
50. Hook, B.A. Paleoclimatology of the Paleocene/Eocene Using Kimberlite-Hosted Mummified Wood from the Canadian Subarctic. Ph.D. Thesis, Department of Earth Sciences, University of Toronto, Toronto, ON, Canada, 2014. 165p.
51. Wolfe, A.P.; Csank, A.Z.; Reyes, A.V.; McKellar, R.C.; Tappert, R. Pristine Early Eocene wood buried deeply in kimberlite from northern Canada. *PLoS ONE* **2012**, *17*, e45537. [[CrossRef](#)] [[PubMed](#)]
52. Hook, B.A.; Halfar, J.; Gedalof, Z.; Bollman, J.; Schulze, D.J. Stable isotope paleoclimatology from the earliest Eocene using kimberlite-hosted mummified wood from the Canadian Subarctic. *Biogeosciences* **2015**, *12*, 5899–5914. [[CrossRef](#)]

53. Hansel, A.K.; Johnson, W.H. *Wedron and Mason Groups: Lithostratigraphic Reclassification of Deposits of the Wisconsin Episode, Lake Michigan Lobe Area*; Illinois State Geological Survey Bulletin 104: Champaign, IL, USA, 1996; 116p.
54. Mossa, J.; Autin, W.J. *Quaternary Geomorphology and Stratigraphy of the Florida Parishes, Southeastern Louisiana: Friends of the Pleistocene, Field Trip Guide Book*; South-Central Cell: Baton Rouge, LA, USA, 1986; pp. 76–94.
55. Yancey, T.E.; Mustoe, G.E.; Leopold, E.B.; Heizler, M.T. Mudflow disturbance in latest Miocene forests in Lewis County, Washington. *PALAIOS* **2013**, *28*, 343–358. [[CrossRef](#)]
56. Mustoe, G.E.; Leopold, E.B. Paleobotanical evidence for the post-Miocene uplift of the Cascade Range. *Can. J. Earth Sci.* **2014**, *51*, 809–824. [[CrossRef](#)]
57. Mickelson, D.M.; Hooyer, T.S.; Soch, B.J.; Winguth, C. Late Glacial ice advances and vegetation changes in east-central Wisconsin. In *Late Glacial History of East-Central Wisconsin*; Survey Open-File Report 2007-1; Hooyer, T.S., Ed.; Wisconsin Geological and Natural History: Madison, WI, USA, 2007; pp. 72–87.
58. Black, R.F. *Glacial Geology of the Two Creeks Forest Bed, Valderan Type Locality, and Northern Kettle Moraine State Forest (Information Circular 13)*; Geological and Natural History Survey, University of Wisconsin: Madison, WI, USA, 1970; pp. 21–30.
59. Goldthwait, J.W. The abandoned shorelines of eastern Wisconsin. *Wis. Geol. Nat. Hist. Surv. Bull.* **1907**, *17*, 1–134.
60. Wilson, L.R. The Two Creeks forest bed, Manitowoc County, Wisconsin. *Trans. Wis. Acad. Sci. Arts Lett.* **1932**, *27*, 31–46.
61. Wilson, L.R. Fossil studies of the Two Creeks forest bed, Manitowoc County, Wisconsin. *Bull. Torrey Bot. Club* **1936**, *63*, 317–325. [[CrossRef](#)]
62. Broecker, W.S.; Farrand, W.R. Radiocarbon age of the Two Creeks Forest bed, Wisconsin. *Geol. Soc. Am. Bull.* **1963**, *74*, 647–649. [[CrossRef](#)]
63. Kaiser, K.F. Two Creeks interstade dated through dendrochronology and AMS. *Quat. Res.* **1994**, *32*, 288–298. [[CrossRef](#)]
64. Panyushkina, I.P.; Leavitt, S.W. Ancient boreal forests under the environmental instability of the glacial to post-glacial transition in the Great Lakes region (14,000–11,000 years BP). *Can. J. For. Res.* **2013**, *3*, 1032–1039. [[CrossRef](#)]
65. Panyshukina, I.P.; Leavitt, S.W.; Mode, W.N. A 1400-Year Bølling-Allerød Tree-Ring Record from the U.S. Great Lakes Region. *Tree-Ring Res.* **2017**, *73*, 102–112. [[CrossRef](#)]
66. Black, R.F.; Geology of the Ice Age Natural Science Reserve of Wisconsin. National Park Service Scientific Monograph No. 2, Chapter 2: Two Creeks Forest Bed 1974. Available online: [https://www.nps.gov/parkhistory/online\\_books/science/2/chap2.htm](https://www.nps.gov/parkhistory/online_books/science/2/chap2.htm) (accessed on 21 April 2018).
67. Panyushkina, I.P.; Leavitt, S.W.; Schneider, A.F.; Thompson, T.A.; Lange, T. Environment and paleoecology of a 12 ka mid-North American Younger Dryas forest chronicled in tree rings. *Quat. Res.* **2008**, *70*, 433–441. [[CrossRef](#)]
68. Panyushkina, I.P.; Leavitt, S.W. Tapping ancient tree-ring archives in the U.S. Great Lakes region. *Eos Trans. Am. Geophys. Union* **2010**, *91*, 489–490. [[CrossRef](#)]
69. Easterbrook, D.J. Stratigraphy and chronology of early to late Pleistocene glacial and interglacial sediments in the Puget Lowland, Washington. In *Geologic Field Trips in the Pacific Northwest, Proceedings of the 1994 Geological Society of America Annual Meeting, Seattle, WA, USA, 24–27 October 1994*; Swanson, D.A., Haugerud, R.A., Eds.; Dept. of Geological Sciences, Univ. of Washington: Seattle, WA, USA, 1994; Volume 1, pp. IJ1–IJ38.
70. Hansen, H.P.; Mackin, J.H. A pre-Wisconsin forest succession in the Puget Lowland, Washington. *Am. J. Sci.* **1949**, *247*, 833–855. [[CrossRef](#)]
71. Easterbrook, D.J.; Crandell, D.R.; Leopold, E.B. Pre-Olympia stratigraphy and chronology in the central Puget Lowland, Washington. *Geol. Soc. Am. Bull.* **1967**, *78*, 13–20. [[CrossRef](#)]
72. Stoffel, K.L. Stratigraphy of pre-Vashon Quaternary sediments applied to the evolution of a proposed major tectonic structure in Island County, Washington. In *Washington Division of Geology and Earth Resources, Open File Report OFR 80-0*; Washington Division of Geology and Earth Resources: Olympia, WA, USA, 1980; 161p.
73. Lechien, V.; Rodriguez, C.; Onenga, M.; Hiligsmann, S.; Rulmont, A.; Thonart, P. Physiochemical and biochemical characterization of non-biodegradable cellulose in Miocene gymnosperm wood from the Entre-Sambre-et-Meuse, southern Belgium. *Org. Chem.* **2006**, *37*, 1465–1476.

74. Simpson, I.M.; West, R.G. On the stratigraphy and palaeobotany of a late-Pleistocene organic deposit at Chelford, Cheshire. *New Phytol.* **1958**, *57*, 239–250. [[CrossRef](#)]
75. Klusik, M.A.; Pawelczyk, S.R. Stable carbon isotope analysis of subfossil wood from the Austrian Alps. *Geochronometria* **2014**, *41*, 400–408.
76. Dorofeyev, P.I. Oligocene flora of the Dunayevsky Crag on the Tym River in western Siberia. *Dokl. Akademii Nauk SSSR* **1960**, *132*, 659–661.
77. Gnibidenko, Z.N.; Semakov, N.N. Paleomagnetism of boundary Oligocene-Miocene deposits in the Kompasski Bor tract on the Tym River (western Siberia). *Izvestia, Phys. Solid Earth* **2009**, *45*, 70–79. [[CrossRef](#)]
78. Kázmér, M. The Miocene Bükkábrány Fossil Forest in Hungary—Field observations and project outline. In *125th Anniversary of the Department of Palaeontology at Budapest University, a Jubilee Volume*; Galácz, A., Ed.. *Hantkeniana* **2008**, *6*, 220–244.
79. Erdei, B.; Dolezych, M.; Hably, L. The buried Miocene forest at Bükkábrány, Hungary. *Rev. Palaeobot. Palynol.* **2009**, *15*, 69–79. [[CrossRef](#)]
80. Gryce, V.; Sakala, J. Identification of fossil trunks from Bükkábrány newly installed in the visitor centre of the Ipolytarnóc Fossils Nature Reserve (Novhrad-Nógrád Geopark) in northern Hungary. *Acta Univ. Agric. Silv. Mendel. Brun.* **2010**, *58*, 117–122. [[CrossRef](#)]
81. Dolezych, M.; Van der Burgh, J. Xylotomische Untersuchungen an inkholten Hölzern aus dem Braunkohlentagebau Berzdorf (Oberlausitz, Deutschland). *Feddes Repert.* **2009**, *115*, 397–437. [[CrossRef](#)]
82. Hámor-Vidó, M.; Hofmann, T.; Albert, L. In Situ preservation and paleoenvironmental assessment of *Taxodiaceae* fossil trees in the Bükkalja Lignite Formation, Bükkábrány open cast mine, Hungary. *Int. J. Coal Geol.* **2010**, *81*, 203–210. [[CrossRef](#)]
83. Baldanza, A.; Sabatino, G.; Triscari, M.; De Angeles, M.C. The Dunarobba Fossil Forest (Umbria, Italy): Mineralogical transformations evidences as possible decay effects. *Per. Mineral.* **2009**, *78*, 51–60.
84. Vassio, E.; Martinetto, E.; Dolezych, M.; Van der Burg, J. Wood anatomy of the *Glyptostrobus europaeus* “whole-plant” from a Pliocene fossil forest in Italy. *Rev. Palaeobot. Palynol.* **2008**, *151*, 81–89. [[CrossRef](#)]
85. Staccioli, G.; Menchi, G.; Matteoli, U.; Seraglia, R.; Traldi, P. Chemotaxonomic observations on some pliocenic woods from Arno Basin and fossil forest of Dunarobba (Italy). *Flora Mediterr.* **1996**, *6*, 113–117.
86. Staccioli, G.; Bartolini, G. New biomarkers of the extinct species *Taxodioxylon gypsaceum*. *Wood. Sci. Technol.* **1997**, *31*, 311–315. [[CrossRef](#)]
87. Staccioli, G.; Fratini, F.; Meli, A.; Lazzeri, S. Mineralization processes in some samples from the fossil forest of Dunarobba (Umbria, Central Italy). *Wood. Sci. Technol.* **2001**, *35*, 353–362. [[CrossRef](#)]
88. Boyce, C.K.; Hazen, R.M.; Knoll, A.H. Nondestructive, in-situ, cellular scale mapping of elemental abundances including organic carbon in permineralized fossils. *Proc. Nat. Acad. Sci. USA* **2001**, *98*, 5970–5974. [[CrossRef](#)] [[PubMed](#)]
89. Scott, A.C.; Collinson, M.E. Non-destructive multiple approaches to interpret the preservation of plant fossils: Implications for calcium-rich permineralizations. *J. Geol. Sci. Lond.* **2003**, *160*, 857–862. [[CrossRef](#)]
90. Martinetto, E.; Bertini, A.; Basilica, G.; Baldanza, A.; Bizzarri, R.; Cherin, M.; Gentili, S.; Pontini, M.R. The plant record of the Dunarobba and Pietrafitta sites in the Plio-Pleistocene palaeoenvironmental context of central Italy. *Alp. Mediter. Quat.* **2014**, *27*, 29–72.
91. Macaluso, L.; Martinetto, E.; Vigna, B.; Bertini, A.; Cilia, A.; Teodordis, V.; Kvaček, S. Palaeofloral and stratigraphic context of a new fossil forest from the Pliocene of NW Italy. *Rev. Palaeobot. Palynol.* **2018**, *248*, 15–33. [[CrossRef](#)]
92. Ambrosetti, P.; Basilici, G.; Ciangherotti, A.D.; Codipietro, G.; Corona, E.; Esu, D.; Girotta, O.; Lo Manco, A.; Meneghina, M.; Paganelli, A.; et al. La Foresta Fossile di Dunarobba (Terni, Umbria, Italia Centrale): Contest lithostratigrafico, sedimentologico, palinologico, dendrochronologico e paleomalacologico. *Ital. J. Quat. Sci.* **1995**, *8*, 465–508.
93. Martinetto, E.; Sardia, G.; Varrone, D. Magnetostratigraphy of the Stura di Lanzo fossil forest succession (Piedmont, Italy). *Riv. Ital. Paleontol. Stratigr.* **2007**, *113*, 109–125.
94. Ferrero, E. Foresta fossile: Fruizione didattica. In *La Foresta Fossile del Torrente Stura di Lanzo. I Quaderni de La Mandria, Ente Parco Regionale La Mandria, Torino*; Martinetto, E., Farina, T., Eds.; Ente di Gestione del Parco Regionale La Mandria e dei Parchi e delle Riserve Naturali delle Valli di Lanzo: Venaria, Italy, 2005; Volume 1, pp. 44–45.

95. Godone, F.; Baaaldo, M.; Maraga, F. Una foresta nell'alveo del F. Stura di Lanzo (TO). Rilevamenti topografici, cartografia e GIS. Atti 8° Conferenza Nazionale ASITA, Roma, 14–17 dic. 2004, Artesanpa sas. *Varese* **2004**, *2*, 1219–1224.
96. Chiariglione, A.; Farina, T.; Ferrero, O.; Forna, M.G.; Gattiglio, M.; Lucchesi, S.; Martinetto, E. La Foresta Fossile dello Stura de Lanzo, Quaderni de la Mandria, Parco La Mandria 2005, 48p. Available online: [https://www.researchgate.net/profile/Edoardo\\_Martinetto](https://www.researchgate.net/profile/Edoardo_Martinetto) (accessed on 19 May 2018).
97. Ferrero, E.; Magagna, A. Natural hazards and geological heritage in Earth science education projects. In *Geoethics: The Role and Responsibility of Geoscientists*; Peppoloni, S., Di Capua, G., Eds.; Geological Society of London Special Publications: London, UK, 2015; p. 419.
98. Ferrero, E.; Gimigliano, D.; Pogliano, A. Educazione ambientale in un'area protetta del territorio piemontese. Il progetto 'La foresta ritrovata'. In Proceedings of the Atti 3rd World Environmental Education Congress, Turin, Italy, 2–6 October 2005; pp. 170–177.
99. Quan, C.; Fu, Q.Y.; Shu, G.L.; Li, Y.S.; Lu, L.; Liu, X.Y.; Jin, J.H. First Oligocene mummified plant Lagerstätte at low latitudes of East Asia. *Sci. China Earth Sci.* **2016**, *59*, 445–560. [[CrossRef](#)]
100. Yamakawa, C.; Momohara, A.; Saito, T.; Nunotani, T. Composition and paleoenvironment of wetland forests dominated by *Glyptostrobus* and *Metasequoia* in the latest Pliocene (2.6Ma) in central Japan. *Palaeogeogr. Palaeoclimatol. Palaeoecol.* **2017**, *467*, 191–210. [[CrossRef](#)]
101. Scott, A.C. The pre-Quaternary history of fire. *Palaeogeogr. Palaeoclimatol. Palaeoecol.* **2000**, *154*, 281–329. [[CrossRef](#)]
102. Scott, A.C.; Cripps, J.A.; Collinson, M.E.; Nicjols, G.J. The taphonomy of charcoal in a Recent heathland fire and some implications for the interpretation of fossil charcoal deposits. *Palaeogeogr. Palaeoclimatol. Palaeoecol.* **2000**, *164*, 1–31. [[CrossRef](#)]
103. Scott, A.C. The preservation of woods in volcanic pyroclastic flows and surges. In Proceedings of the Geological Society of America 2001 Annual Meeting, Boston, MA, USA, 5–8 November; p. 68.
104. Scott, A.C. Charcoal recognition, taphonomy, and uses in paleoenvironmental analysis. *Palaeogeogr. Palaeoclimatol. Palaeoecol.* **2010**, *291*, 11–39. [[CrossRef](#)]
105. Scott, A.C.; Damblon, F. Charcoal: Taphonomy and significance in geology, botany, and archaeology. *Palaeogeogr. Palaeoclimatol. Palaeoecol.* **2010**, *291*, 1–10. [[CrossRef](#)]
106. Sander, O.M.; Gee, C.T. Fossil charcoal: Techniques and applications. *Rev. Palaeobot. Palynol.* **1990**, *63*, 269–279. [[CrossRef](#)]
107. Glasspool, I.J.; Scott, A.C. Phanerozoic concentrations of atmospheric oxygen reconstructed from sedimentary charcoal. *Nat. Geosci.* **2010**, *3*, 627–630. [[CrossRef](#)]
108. Moore, P.R.; Wallace, R. Petrified wood from the Miocene volcanic sequence of Coromandel Peninsula, northern New Zealand. *J. R. Soc. N. Z.* **2000**, *30*, 115–130. [[CrossRef](#)]
109. Hudspeth, V.A.; Scott, A.C.; Wilson, C.J.N.; Collinson, M.E. Charring of woods by volcanic processes: An example from the Taupo ignimbrite, New Zealand. *Palaeogeogr. Palaeoclimatol. Palaeoecol.* **2010**, *291*, 40–51. [[CrossRef](#)]
110. Glasspool, I.J.; Edwards, D.; Axe, L. Charcoal in the Silurian as evidence for the earliest wildfire. *Geology* **2004**, *32*, 381–383. [[CrossRef](#)]
111. Glasspool, I.J.; Edwards, D.; Axe, L. Charcoal in the Early Devonian: A wildfire-derived Konservate-Lagerstätte. *Rev. Paleobot. Palynol.* **2006**, *142*, 131–136. [[CrossRef](#)]
112. Prestianni, C.; Decombeix, A.L.; Thorez, J.; Fokan, D.; Gerrienne, P. Famennian charcoal of Belgium. *Palaeogeography* **2010**, *291*, 60–71. [[CrossRef](#)]
113. Berner, R.Z.; Canfield, D.E. A new model for atmospheric oxygen over Phanerozoic time. *Am. J. Sci.* **1989**, *289*, 333–361. [[CrossRef](#)] [[PubMed](#)]
114. Berner, R.A.; Beerling, D.J.; Dudley, R.; Robinson, J.M.; Wildman, R.A., Jr. Phanerozoic atmospheric oxygen. *Annu. Rev. Earth Planet. Sci.* **2003**, *31*, 105–134. [[CrossRef](#)]
115. Berner, R.A. The carbon and sulfur cycles and atmospheric oxygen from Middle Permian to late Triassic. *Geochim. Cosmochim. Acta* **2005**, *69*, 3211–3217. [[CrossRef](#)]
116. Jones, T.P.; Chaloner, W.H. Fossil charcoal, its recognition and paleoatmospheric significance. *Palaeogeogr. Palaeoclimatol. Palaeoecol.* **1991**, *97*, 39–50. [[CrossRef](#)]
117. Tanner, L.H.; Wang, X.; Morabito, A.C. Fossil charcoal from the Middle Jurassic of the Ordos Basin, China and its paleoatmospheric implications. *Geosci. Front.* **2012**, *3*, 493–502. [[CrossRef](#)]

118. Belcher, C.M.; Yearsle, J.M.; Hadden, R.M.; McElwaine, J.C.; Rein, G. Baseline intrinsic flammability of Earth's exosystems estimated from paleoatmospheric oxygen over the past 350 million years. *PNAS* **2010**, *107*, 22448–22543. [[CrossRef](#)] [[PubMed](#)]
119. Uhl, D.; Dolezych, M.; Böhme, M. *Taxodioxylon*-like charcoal from the Late Miocene of western Bulgaria. *Acta Palaeontol.* **2014**, *54*, 101–111.
120. McPartland, L.C.; Collinson, M.E.; Scott, A.C.; Steart, D.C.; Grassineau, N.V.; Gibbins, S.J. Ferns and fires: Experimental charring of ferns compared to wood and implications for paleobiology, paleoecology, coal petrology, and isotope geochemistry. *PALAIOS* **2007**, *22*, 528–538. [[CrossRef](#)]
121. Byers, B.A.; Ash, S.R.; Chaney, D.; DeSoto, L. First known fire scar on a fossil tree trunk provides evidence of Late Triassic wildfire. *Palaeogeogr. Palaeoclimatol. Palaeoecol.* **2014**, *411*, 180–187. [[CrossRef](#)]
122. Stout, S.A.; Brown, J.J.; Packman, W. Molecular aspects of the peatification and early coalification of angiosperm and gymnosperm woods. *Geochim. Cosmochim. Acta* **1988**, *52*, 405–414. [[CrossRef](#)]
123. Rodgers, R.E.; Ramurthy, M.; Rodvelt, G.; Mullin, M. *Coalbed Methane, Principles and Practices*, 3rd ed.; Oktibbeha Pub. Co.: Starkville, MS, USA, 2007; pp. 97–98.
124. Ravazzi, C.; Van der Burgh, J. Coniferous woods in the early Pleistocene brown coals of the Lefte Basin (Lombardy, Italy). *Riv. It. Paleont. Strat.* **1995**, *100*.
125. Dolezych, M. Taxodiaceous woods in Lusatia (central Europe), including curiosities in their nomenclature and taxonomy, with a focus on *Taxodioxylon*. *Jpn. J. Hist. Bot.* **2011**, *19*, 25–46.
126. Dolezych, M. A remarkable extinct wood from Lusatia (central Europe)—*Juniperoxylon schneiderianum* sp. Nov. with affinity to *Cupressospermum saxonicum* MAI. *Palaeontogr. Abt. B Palaeobot.-Paleoepiphytol.* **2016**, *295*, 5–31.
127. Nestler, K.; Deitrich, D.; Witke, K.; Rößler, R.; Marx, G. Thermogravimetric and Raman spectroscopic investigations on different coals in comparison to dispersed anthracite found in permineralized tree fern *Psaronius* sp. *J. Mol. Struct.* **2003**, *661–662*, 357–362. [[CrossRef](#)]
128. Hedges, J.I.; Cowie, G.L.; Ertel, J.R.; Barbour, R.J.; Hatcher, P.G. Degradation of carbohydrates and lignins in buried woods. *Geochim. Cosmochim. Acta* **1985**, *49*, 700–711. [[CrossRef](#)]
129. Bestland, E. Volcanic stratigraphy of the Oligocene Colestin Formation in the Siskiyou Pass area of southern Oregon. *Or. Geol.* **1987**, *49*, 79–86.
130. Williams, C.J.; Trostle, K.D.; Sunderlin, D. Fossil wood in coal-forming environments of the Late Paleocene–Early Eocene Chickaloon Formation. *Palaeogeogr. Palaeoclimatol. Palaeoecol.* **2010**, *295*, 363–375. [[CrossRef](#)]
131. Sweeney, I.J.; Chin, K.; Hower, J.C.; Budd, D.A.; Wolfe, D.G. Fossil wood from the middle Cretaceous Moreno Hill Formation: Unique expressions of wood mineralization and implications for the processes of wood preservation. *Int. J. Coal Geol.* **2009**, *79*, 1–17. [[CrossRef](#)]
132. Havelcová, M.; Sýkorová, I.; Bectel, A.; Mach, K.; Trejtnarová, H.; Žaloudková, M.; Matusová, P.; Blažek, J.; Boudová, J.; Sakala, J. “Stump Horizon” Bílina Mine (Most Basin, Czech Republic)-GC-MS, optical and electron microscopy in identification of wood of biological origin. *Int. J. Coal Geol.* **2013**, *107*, 62–77. [[CrossRef](#)]

